Turbulence and its control: hints from Reversed Field Pinch plasmas

V.Antoni

Consorzio RFX, Associazione Euratom_ENEA sulla Fusione, Italy

Outline

Reversed Field Pinch (RFP) configuration: main features & experiments

Magnetic configuration self-organization : dynamo, magnetic turbulence & chaos in the core region (review)

Edge turbulence self-regulation: ExB flow shear, anomalous transport & coherent structures (review & latest results)

Techniques applied for electrostatic turbulence control

Future work

RFP configuration

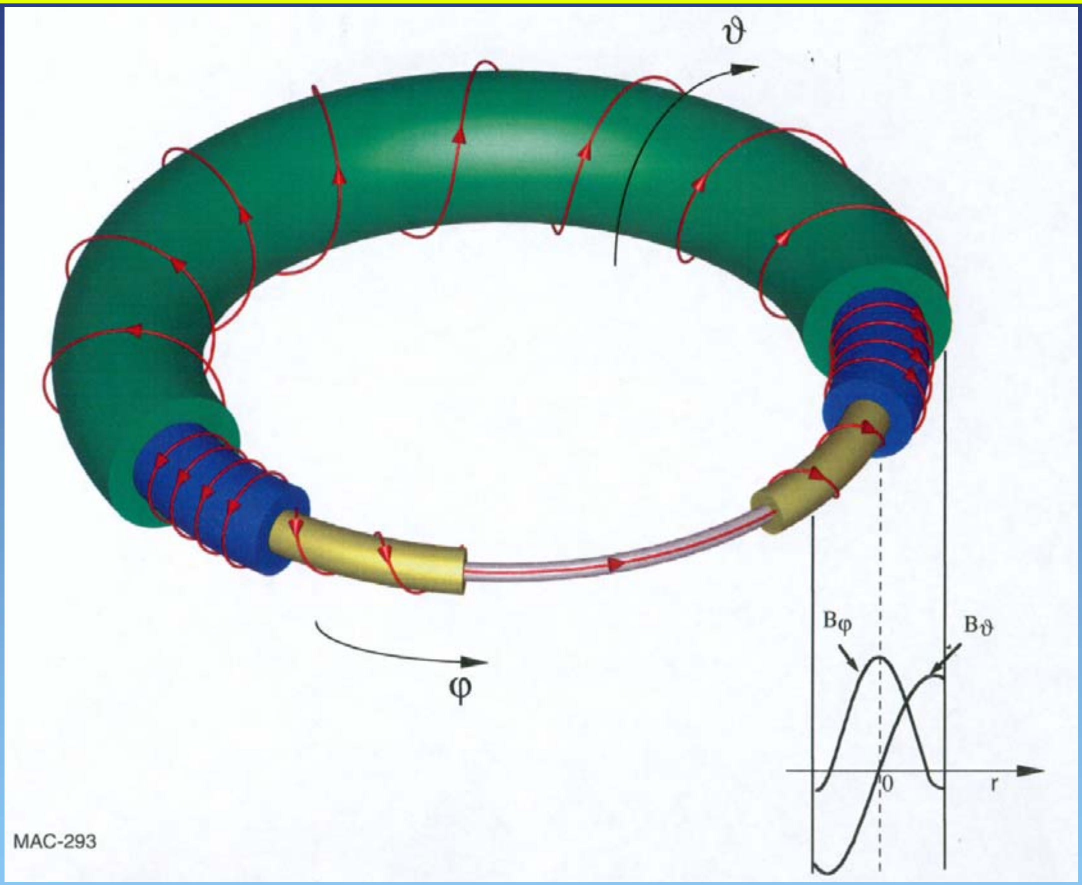

Magnetic field mainly produced by internal currents

Toroidal field changes sign at the edge

Sustaining the toroidal current results in whole configuration sustainment including poloidal currents at the plasma periphery (Dynamo mechanism)

RFP Experiments

RFX
(Consorzio RFX - Padua)

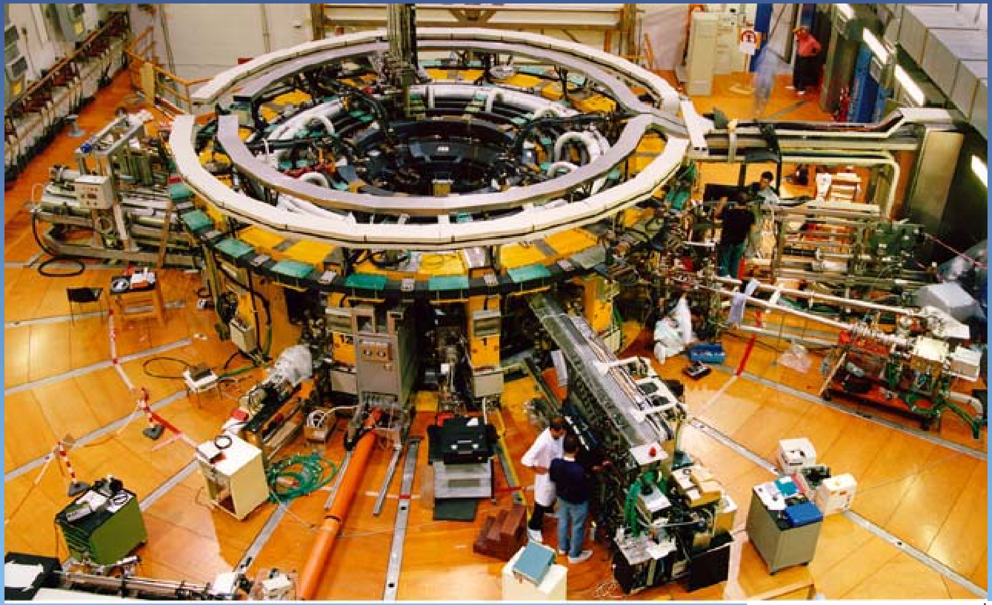

R = 2 m
a = 0.46 m

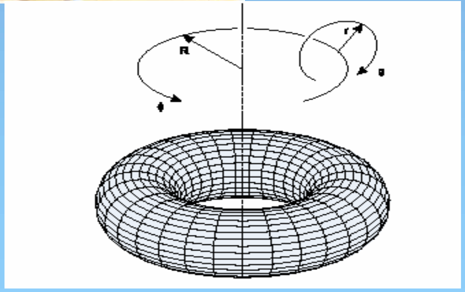

T2R
(KTH - Stockholm)

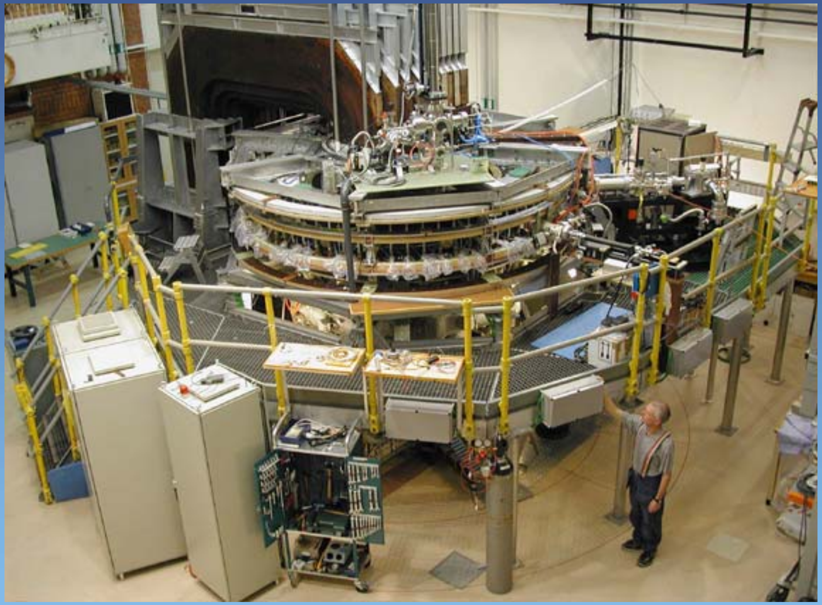

R = 1.24 m
a = 0.183 m

RFP: core and edge regions

The B_ϕ reversal surface separates two distinct regions: core region and edge region

In the core region MHD modes determine dynamics (Dynamo) and transport

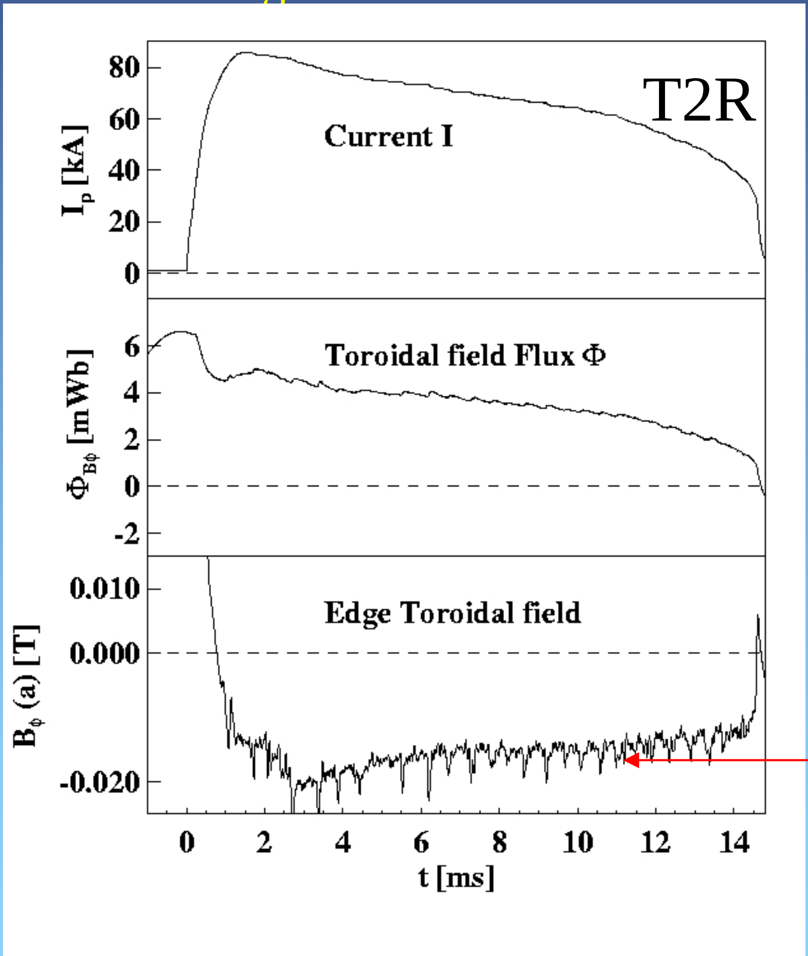

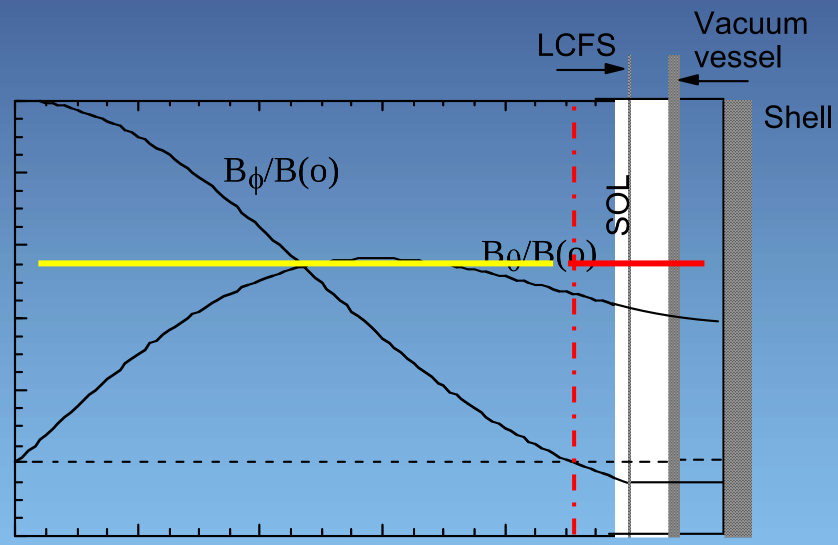

Dynamo manifests with periodic oscillations due to the counteracting actions of resistive diffusion and magnetic relaxation due to MHD instabilities.

RFP: core region

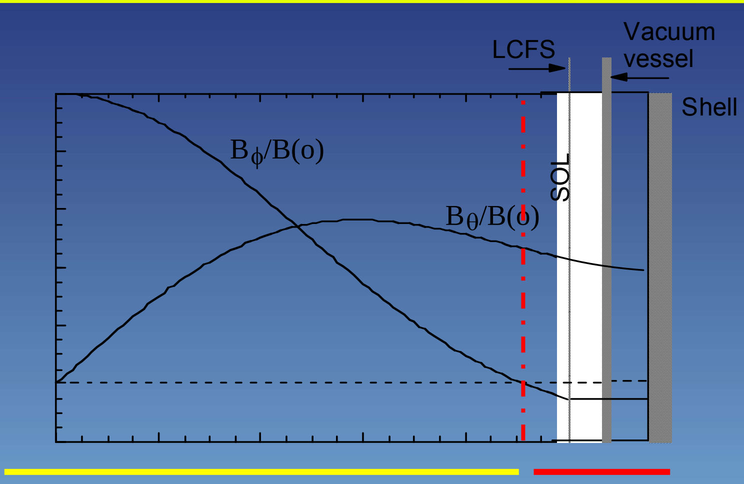

Magnetic configuration characteristics:

High magnetic shear for r/a>0.5
Safety factor q <1
Several m=1 resonant surfaces present
Resonant surface for m=0 at the B_ϕ reversal surface

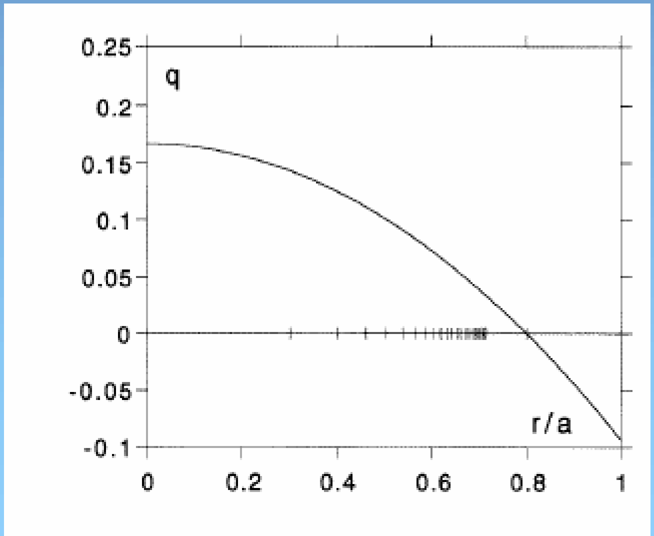

modes *m* = 0 (linearly stable with a close ideal boundary) are nonlinearly driven by most unstable *m* = 1 modes

RFP: MHD dynamics and dissipative forces

The RFP dynamics is described by

$$\frac{\partial \mathbf{B}}{\partial t} = \nabla \times (\mathbf{v} \times \mathbf{B} - \eta \mathbf{J})$$

$$\frac{\partial \mathbf{v}}{\partial t} + (\mathbf{v} \cdot \nabla)\mathbf{v} = \mathbf{J} \times \mathbf{B} + \nu \nabla^2 \mathbf{v}$$

Normalizing, the equations become:

$$\frac{\partial \mathbf{B}}{\partial \bar{t}} = \nabla \times (\bar{\mathbf{v}} \times \mathbf{B} - H^{-1} \mathbf{J})$$

$$P^{-1} \left[\frac{\partial \bar{\mathbf{v}}}{\partial \bar{t}} + (\bar{\mathbf{v}} \cdot \nabla)\bar{\mathbf{v}} \right] = \mathbf{J} \times \mathbf{B} + H^{-1} \nabla^2 \mathbf{v}$$

where

$H = 1/\nu\eta$ is the Hartmann number

$P = \nu/\eta$ is the magnetic Prandtl number

ν=plasma viscosity

η= plasma resistivity

Turbulent & laminar regimes

Two different regimes are predicted in RFP: Laminar and turbulent regimes

Turbulent regimes or Multi Helicity (MH) regimes are characterized by an axisymmetric configuration whose symmetry is broken by intense MHD turbulence

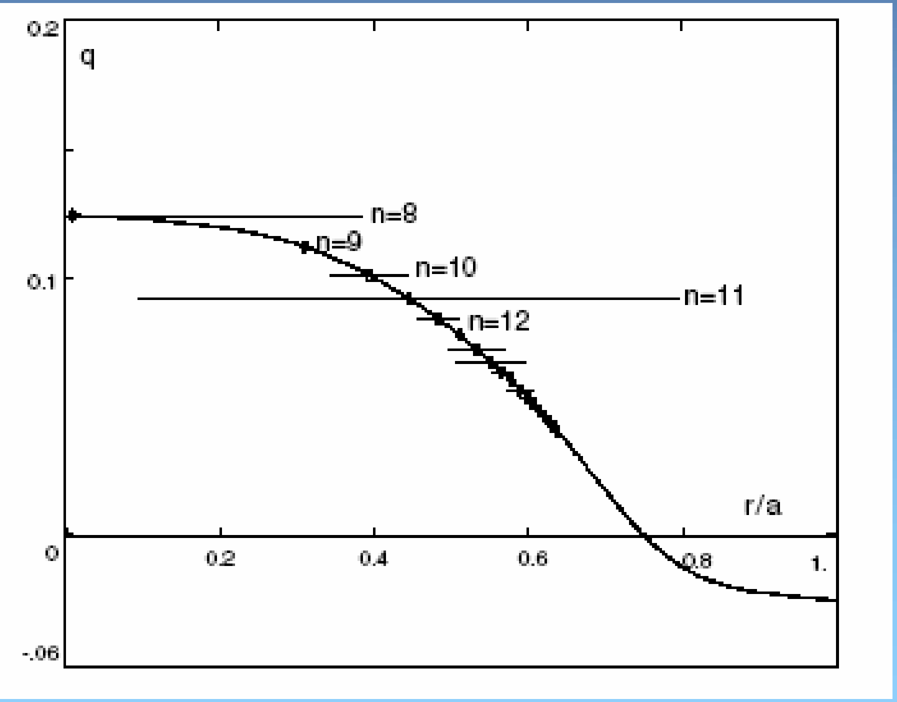

Laminar regimes or Single (SH) and Quasi-Single Helicity (QSH) regimes are characterized by a helical symmetric configuration whose symmetry may be broken by small MHD perturbation.

S. Cappello, EPS 2004
to be published in
PPFC (2004)

Regime transition

The transition from Turbulent to Laminar regimes depends on dissipative forces and in particular on the Hartmann number H:

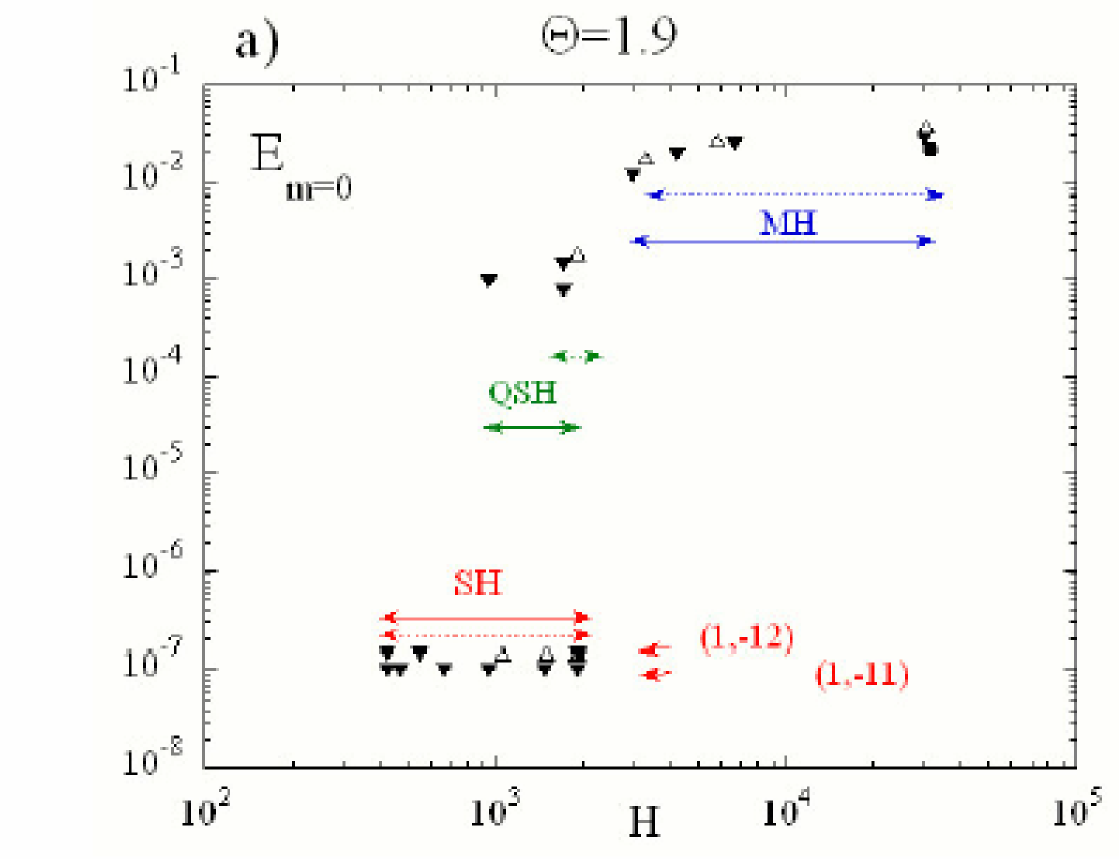

S. Cappello, EPS 2004 to be published in PPFC (2004)

m = 0 mode energy is used as an order parameter to characterize the dynamical regimes
Experimentally only MH and QSH regimes have been observed so far.

Magnetic stochasticity in the core region

In a Multi Helicity (turbulent) regime , the interaction of several m=1 modes results in a completely stochastic core

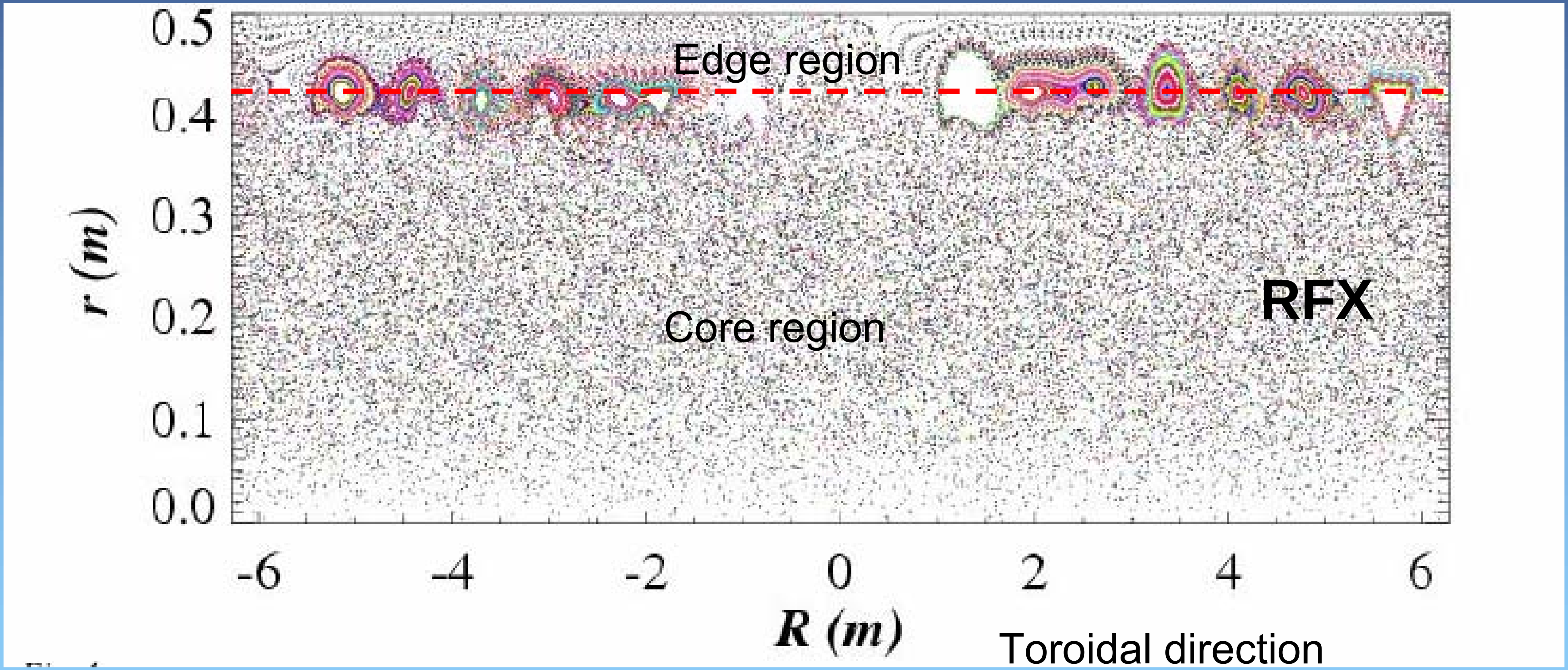

Caos healing

Chaos healing has been predicted when a dominant symmetry emerges in the plasma.
Poincaré plot show that increasing the evergy of the dominant mode, the magnetic separatrix is expelled and chaos reduced

D.F. Escande, et al, *PRL* **85** 3169 (2000)

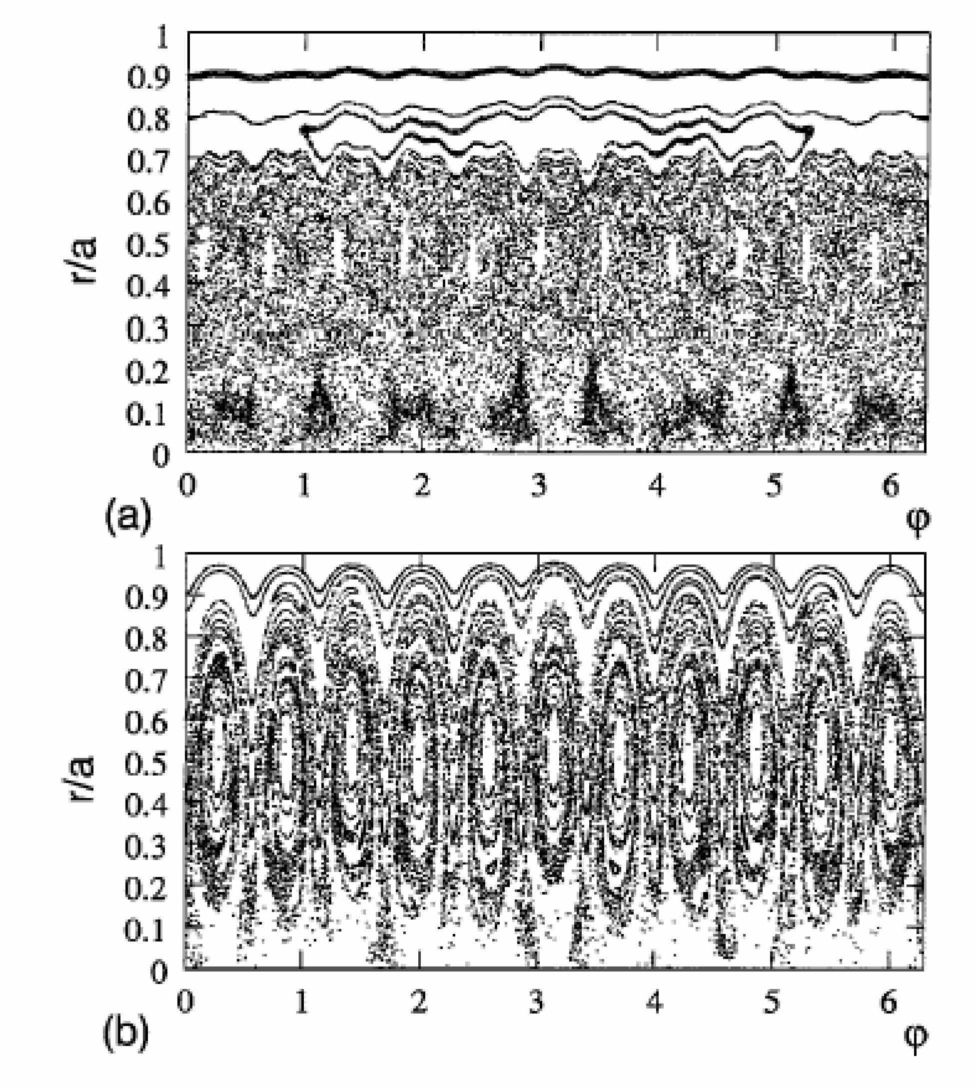

Dynamo electric field in the edge region

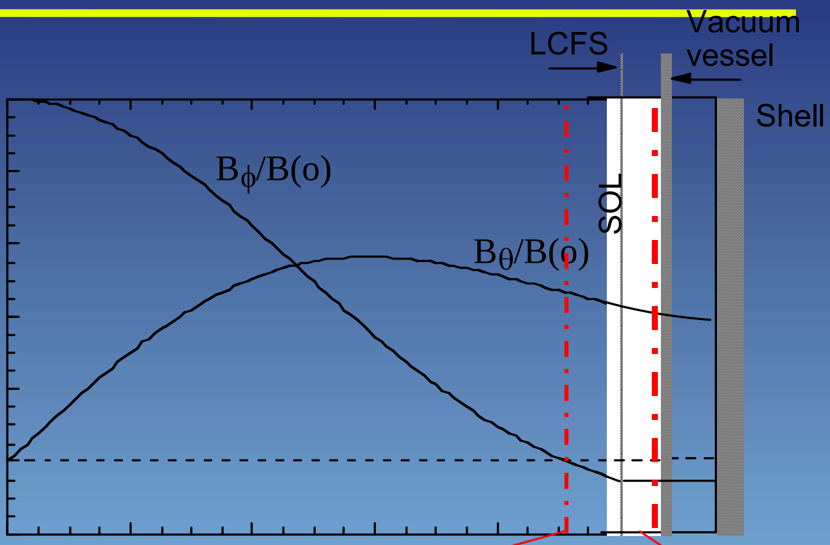

A Dynamo Electric Field
is established in the outer region
The Dynamo electric field is due to the coupling of velocity and magnetic fluctuations

$$E_D = \langle \tilde{v} \times \tilde{b} \rangle$$

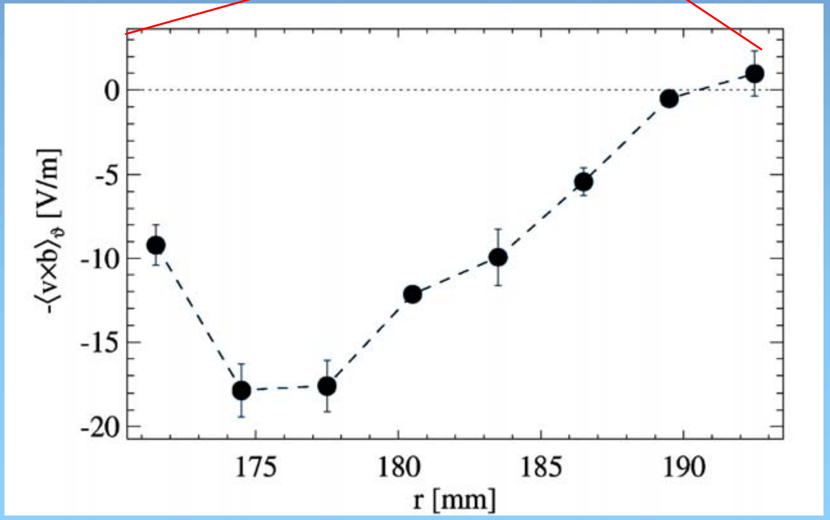

The experimental dynamo E has been measured in T2R (in a MH regime)

Edge parameters

RFX

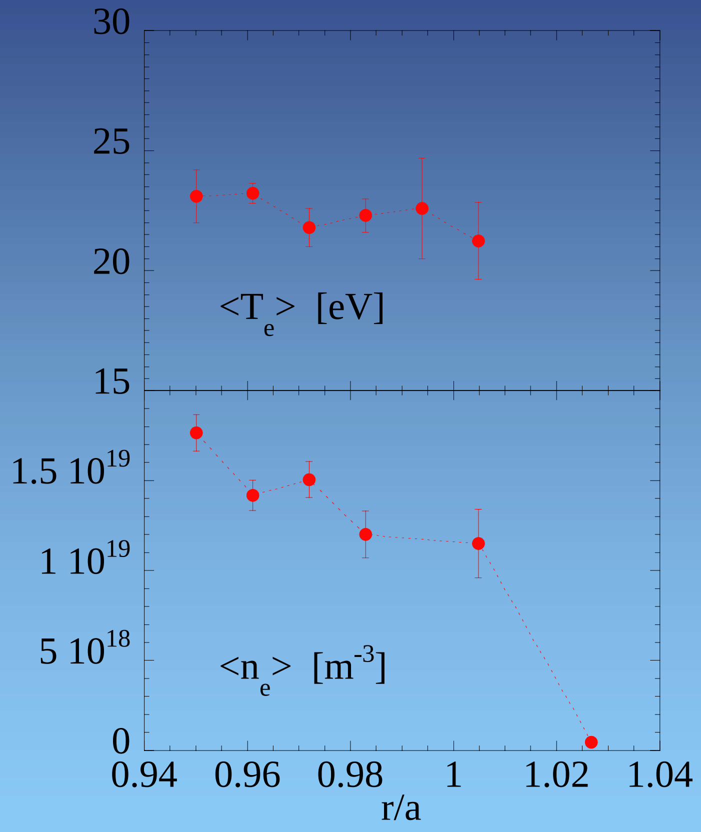

T~ 20 eV
$n \sim 10^{19} m^{-3}$

T2R

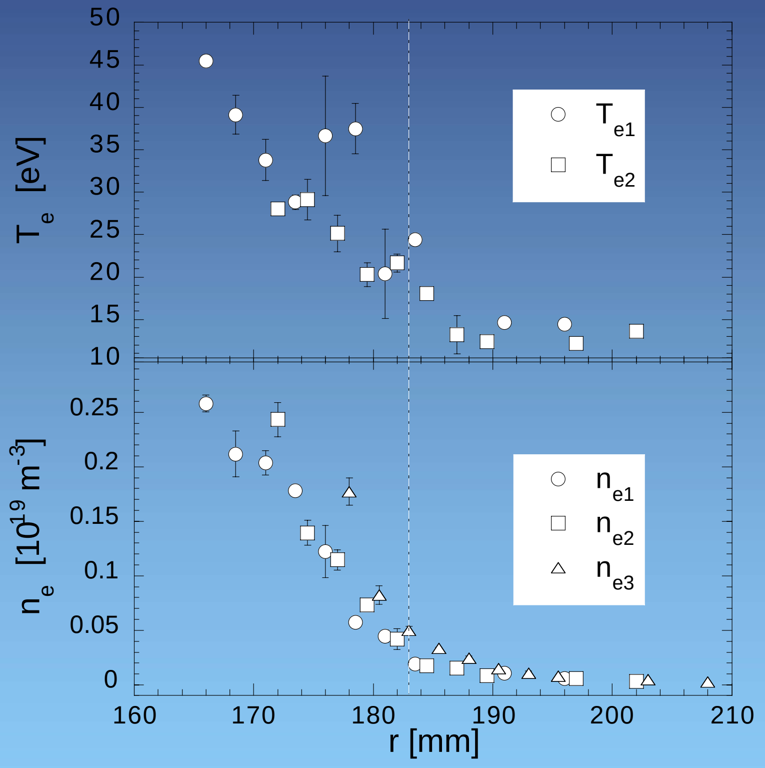

T~ 30 eV
$n \sim 10^{18} m^{-3}$

Turbulence characteristics: fluctuation amplitude and k,f spectra

Typical normalised fluctuation levels are $\delta T/T \sim 30\%$ $\delta n/n \sim 50\%$ and $\delta V/T \sim 100\%$

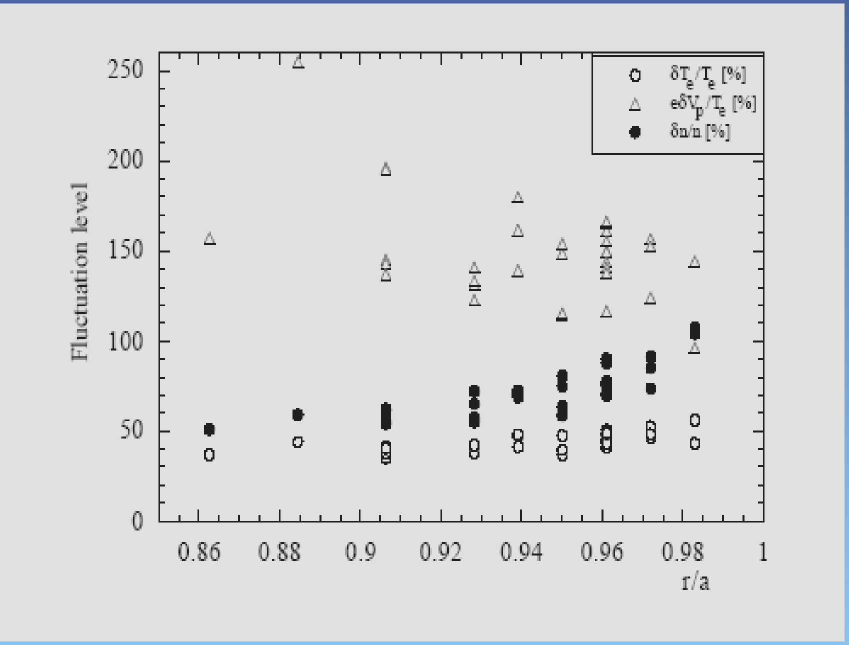

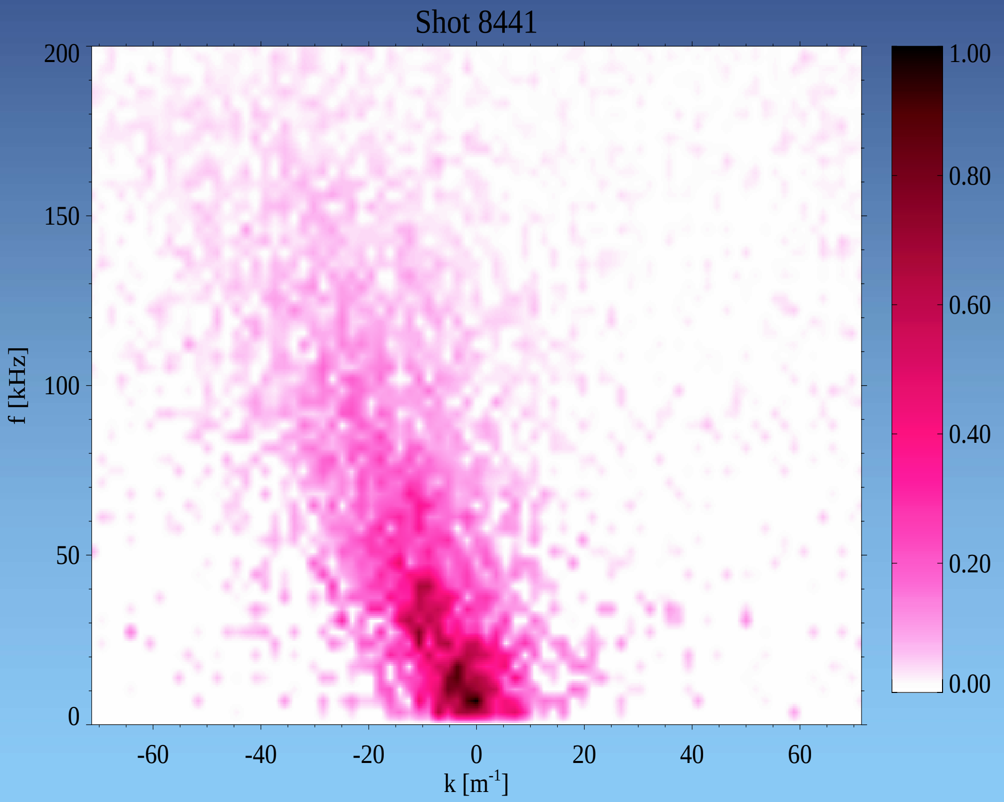

$$\frac{\tilde{T}}{\overline{\overline{T}}} < \frac{\tilde{n}}{\overline{n}} < \frac{\tilde{\phi}}{\overline{\overline{T}}}$$

Electrostatic turbulence has broadband features

Δt = 10.0 - 40.0 ms
Δμ = 0 - 9999 kHz
\FLIP_A2A4_V
\FLIP_C1_V
N_{slices} = 100 N_k = 81

13 Oct 1997
11:19:20

RFP: Particle transport at the edge

Turbulence carries most of the particle flux at the edge (as in tokamaks and stellarators)

RFX

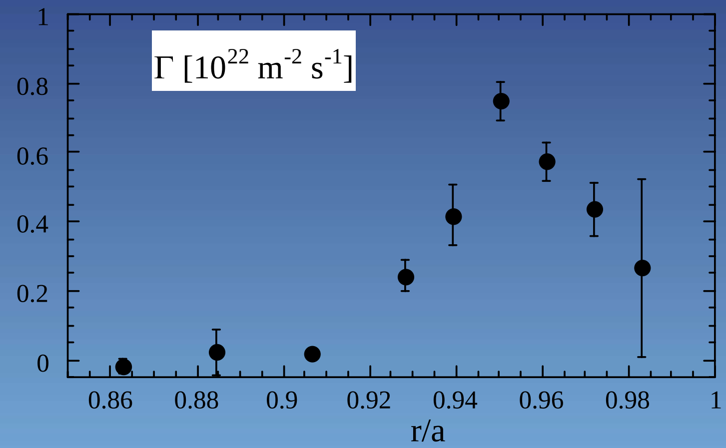

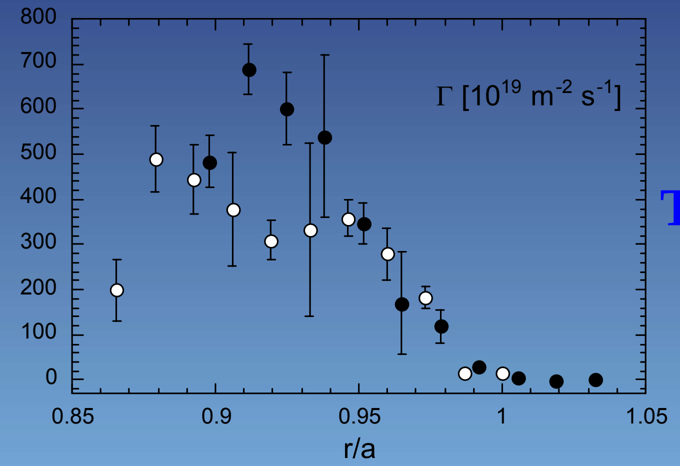

T2R

The effective diffusion coefficient, $D = \Gamma_{es} / \nabla n$ is comparable or larger than the Bohm diffusion

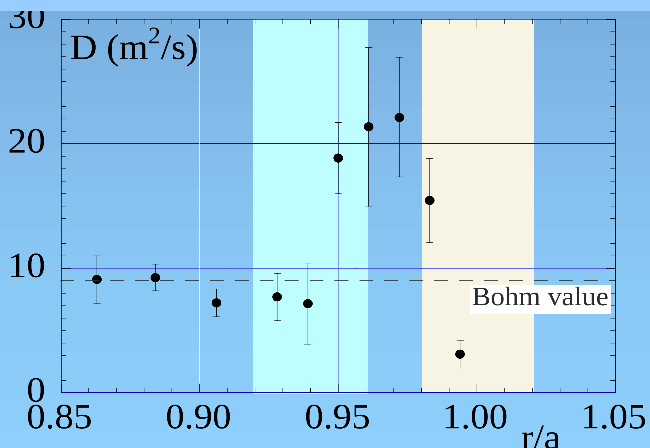

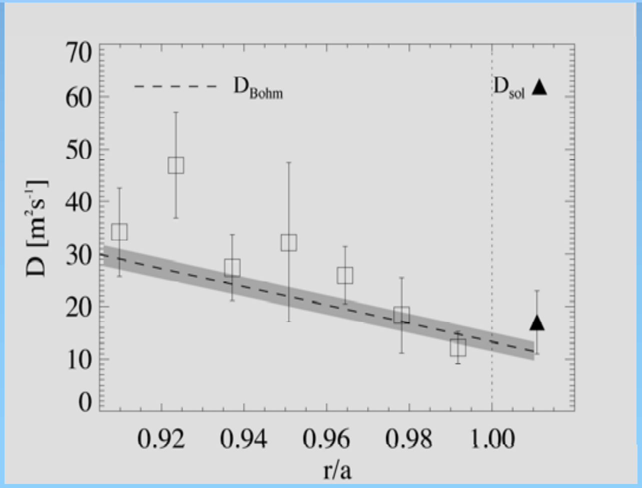

Plasma Phys. Control. Fusion 42 (2000) 83

Particle flux: frequencies and wave-vectors

RFX

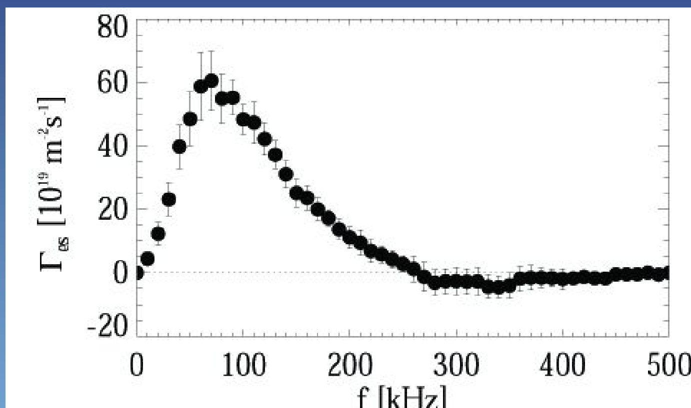

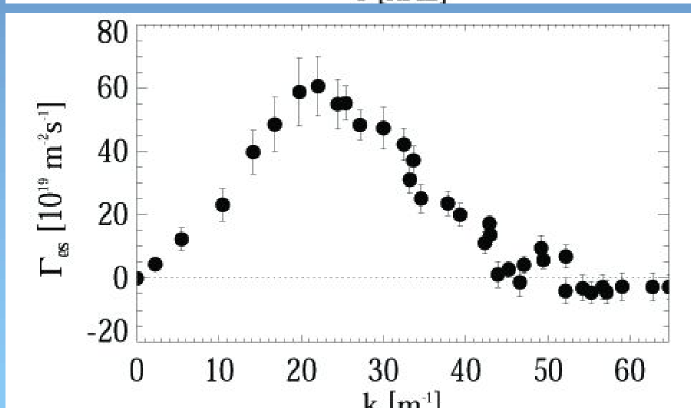

Time scale range: $5 < \tau < 50$ μs

Wave-length range: $0.15 < \lambda < 1$ m

T2R

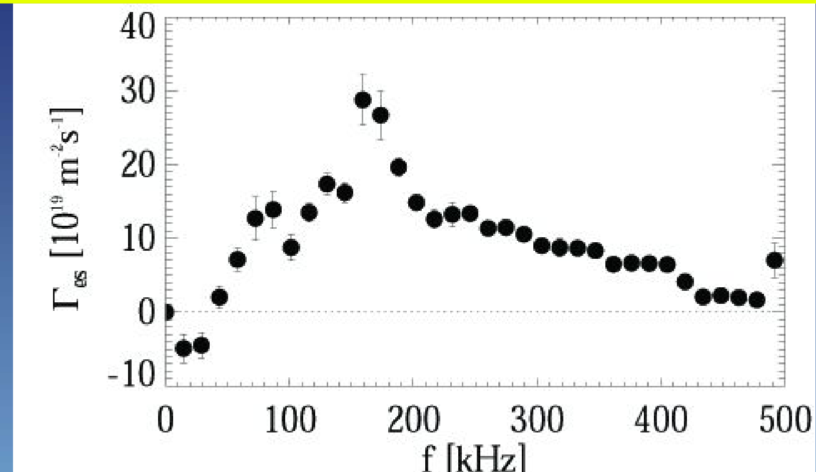

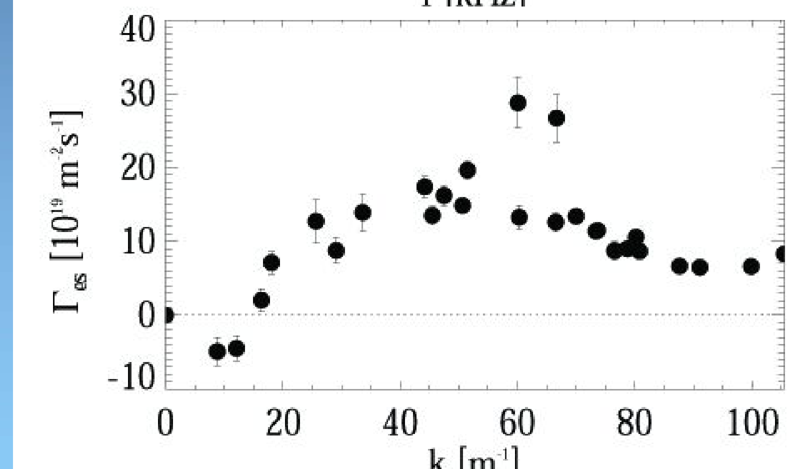

Time scale range: $2.5 < \tau < 20$ μs

Wave-length range: $0.06 < \lambda < 0.6$ m

Particle flux relevant frequencies and wave-vectors

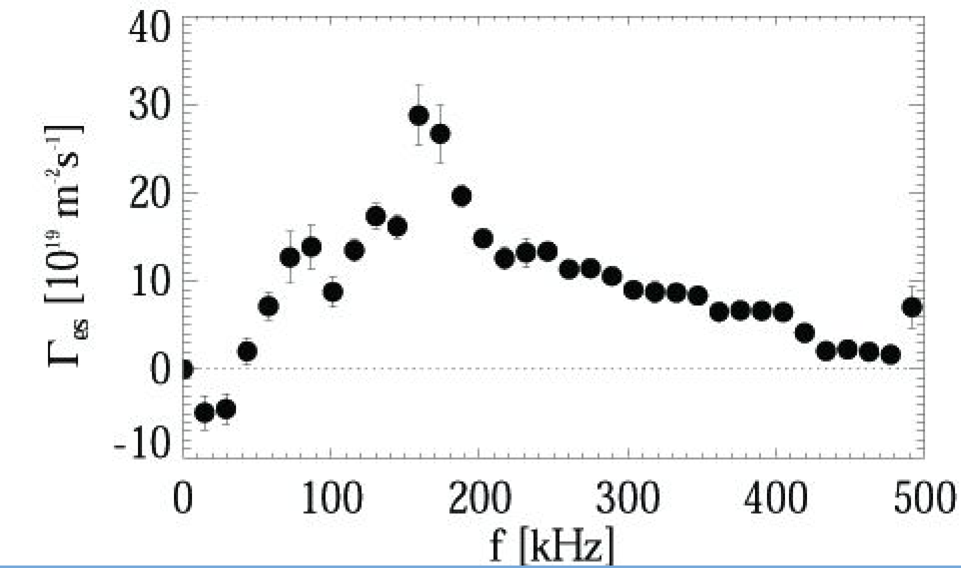

T2R

$2.5 < \tau < 20\ \mu s$
$0.06 < \lambda < 0.6$ m

Time scale range: $2.5 < \tau < 20\ \mu s$

Toroidal wave-length range: $0.06 < \lambda < 0.6$ m

Characteristic frequency & length:

Confinement times 300μs
MHD frequency <80kHz
Ion cyclotron frequency ~1MHz
Major circumference ~ 7 m
Larmor radius ~ 10^{-2} m

ExB velocity in the edge region

RFX B_θ=0.12 T

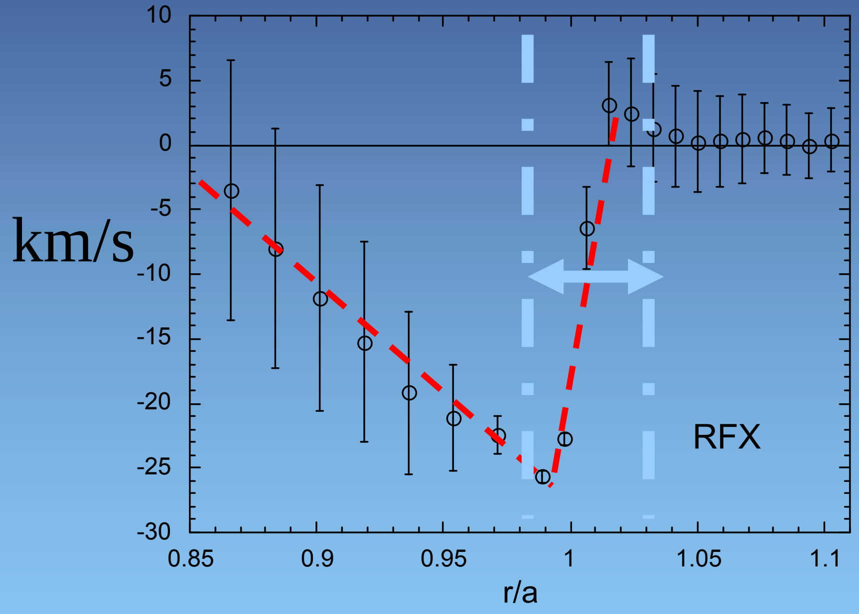

T2R B_θ=0.08 T

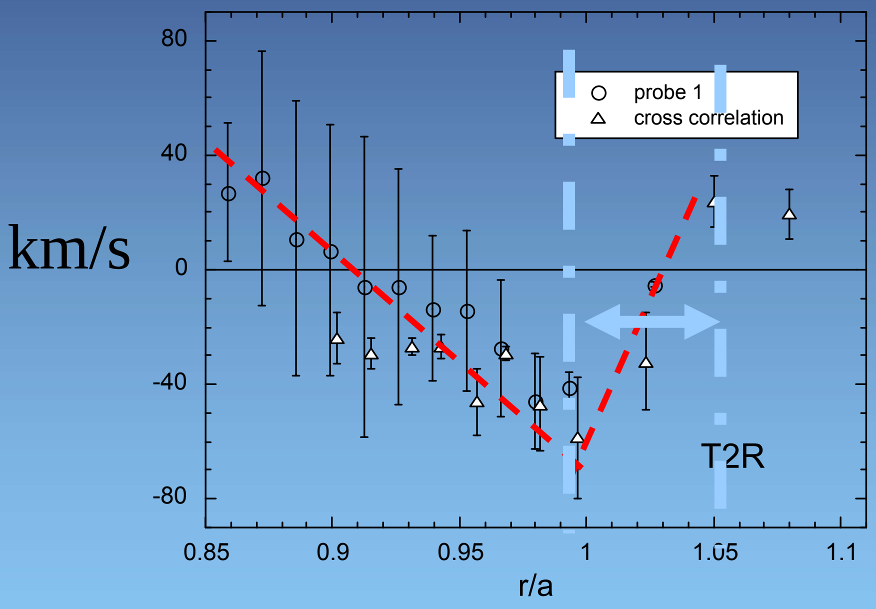

The radial E gives rise to a ExB drift velocity in the toroidal direction (B is mainly poloidal) with a relatively high shear which changes sign in a narrow region. The width of the shear closer to wall has width comparable to a Larmor radius

Phys. Rev. Lett. 79, 4814 (1997).

The Biglari-Diamond-Terry (BDT) criterion

BDT criterion for turbulence decorrelation

H. Biglari, P.H.Diamond, P.W.Terry, Phys. Fluids B 2 (1990) 1

$\omega_s > \Delta\omega_t$

where $\omega_s = k\,\Delta r_t\; dv_{E\times B}/dr$

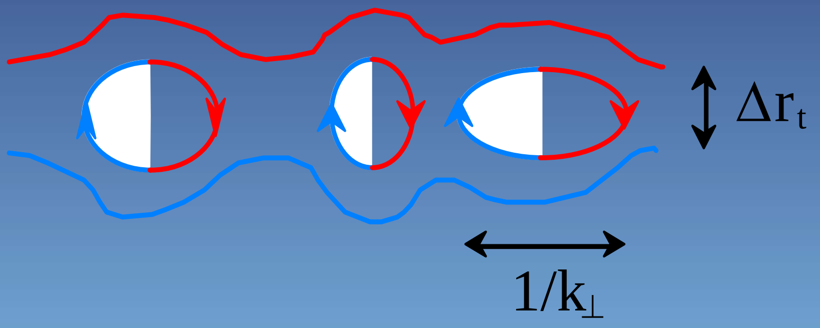

Where

ω_s =shearing frequency

Δr_t = turbulence radial correlation length

k= turbulence wavevector

$\Delta\omega_t$ =ambient turbulence spectrum width

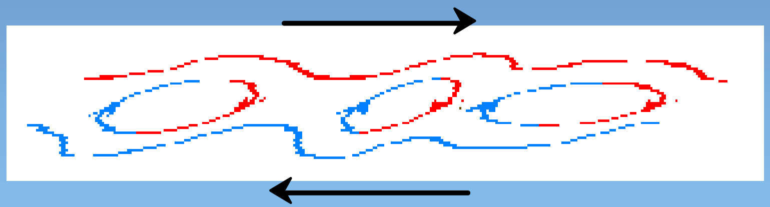

Experimental flow shear and BDT model

In the RFX second velocity shear layer:

$\Delta\omega_t \sim (3.3 \pm 0.3) \cdot 10^5$ rad/s

$k = 12 \pm 2\ m^{-1}$
$dv_{E\times B}/dr = (1.1 \pm 0.4) \cdot 10^6\ s^{-1}$
$\Delta r_m = 1.2 \pm 0.5$ cm(measured by reflectometer)

$\omega_s \sim (1.6 \pm 0.9) \cdot 10^5$ rad/s

In the T2R second velocity shear layer:

$\Delta\omega_t \sim (1.5) \cdot 10^6$ rad/s

$k \sim 50 \pm 2\ m^{-1}$
$dv_{E\times B}/dr \sim (3.8) \cdot 10^6\ s^{-1}$
$\Delta r_m \sim 1.4$ cm(measured by floating potential)

$\omega_s \sim (3.1 \pm 0.9) \cdot 10^6$ rad/s

In RFX and T2R the spontaneous ExB shear gives a shearing frequency ω_s comparable to the turbulence characteristic time scale $\Delta\omega_t$ so that the spontaneous shear in the RFP results marginal for turbulence stabilisation.

Phys. Rev. Lett. 80, 4185 (1998).

Momentum equation for a compressible plasma

Momentum equation

$$\rho\left(\frac{\partial}{\partial t}+\mathbf{V}\cdot\nabla\right)\mathbf{V}=-\nabla\mathbf{P}+\mu\nabla^2\mathbf{V}+\mathbf{J}\times\mathbf{B}$$

Continuity equation

$$\frac{\partial n}{\partial t}+\nabla\cdot(n\mathbf{V})=\nabla\cdot\Gamma^0$$

Substituting **J**

$$\mu_0\vec{J}=\nabla\times\vec{B}$$

Approximations: cylindrical geometry and curvature effects negligible

Momentum balance

The toroidal component of the momentum equation (neglecting curvature and assuming θ and ϕ symmetry) reads for a compressible plasma (friction with neutrals small)

$$\frac{\partial(\rho V_\phi)}{\partial t} + \partial_r\left(\rho V_r V_\phi - \frac{B_r B_\phi}{\mu_0}\right) = \mu\partial_r^2 V_\phi + m_i \partial_r \Gamma^0 V_\phi$$

Dividing each field into average quantities and fluctuating part

$$\mathbf{V} = \overline{\mathbf{V}} + \tilde{\mathbf{v}} \quad \mathbf{B} = \overline{\mathbf{B}} + \tilde{\mathbf{b}} \quad \rho = \overline{\rho} + \tilde{\rho}$$

…and ensemble averaging the equation:

$$\frac{\partial\langle\rho V_\phi\rangle}{\partial t} + \frac{\partial}{\partial r}\left[-\overline{\rho}\langle\frac{\tilde{b}_r\tilde{b}_\phi}{\overline{\rho}\mu_0} - \tilde{v}_r\tilde{v}_\phi\rangle + \langle\tilde{\rho}\tilde{v}_r\rangle\overline{V}_\phi + \langle\tilde{\rho}\tilde{v}_\phi\rangle\overline{V}_r + \langle\tilde{v}_r\tilde{v}_\phi\tilde{\rho}\rangle\right] =$$
$$-\frac{\partial}{\partial r}\left(\overline{\rho}\,\overline{V}_r\overline{V}_\phi - \frac{\overline{B}_r\overline{B}_\phi}{\mu_0}\right) + \mu\frac{\partial^2\overline{V}_\phi}{\partial r^2} + m_i\frac{\partial\overline{\Gamma}_r^0}{\partial r}\overline{V}_\phi$$

Diagnostics in T2R

$$V \approx \frac{E \times B}{B^2} \qquad \tilde{v} = \frac{\tilde{E} \times B}{B^2}$$

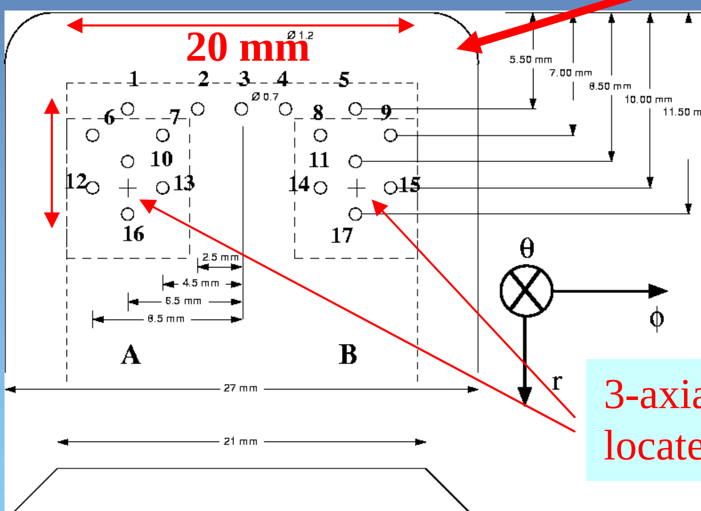

3-axial magnetic probes located in A and B

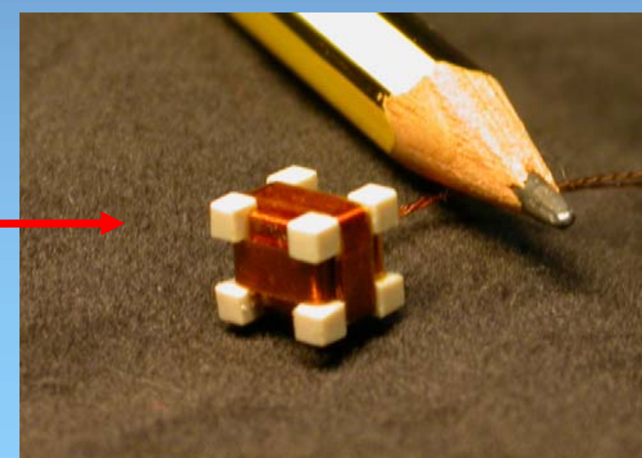

17 electrostatic pins , 0.6 mm diameter, protruding of 1.5 mm from the boron nitride case

Momentum balance

Experimental results have allowed the equation to be simplified as in stationary condition:

$$\nabla \cdot \Gamma_{es} = \nabla \cdot (\langle \tilde{n}_e \tilde{v}_r \rangle) = \nabla \cdot \Gamma^0$$

$$\overline{B}_r = 0$$

Terms containing $\overline{V}_r$ result negligible

$$\frac{\partial}{\partial r}\left[\underbrace{-\overline{\rho}\langle \frac{\tilde{b}_r \tilde{b}_\phi}{\overline{\rho}\mu_0} - \tilde{v}_r \tilde{v}_\phi \rangle}_{A} + \underbrace{\langle \tilde{v}_r \tilde{v}_\phi \tilde{\rho} \rangle}_{B}\right] + \underbrace{m_i \Gamma_{es} \frac{\partial \overline{V}_\phi}{\partial r}}_{C} \approx \mu \frac{\partial^2 \overline{V}_\phi}{\partial r^2}$$

Reynolds Stress (RS)

$$RS = -\langle \tilde{v}_r \tilde{v}_\phi \rangle + \frac{\langle \tilde{b}_r \tilde{b}_\phi \rangle}{\bar{\rho}\mu_0}$$

✓RS has comparable electrostatic and magnetic component

✓RS exhibits a strong radial gradient where velocity is highly sheared

✓The RS gradient is mostly due to electrostatic component

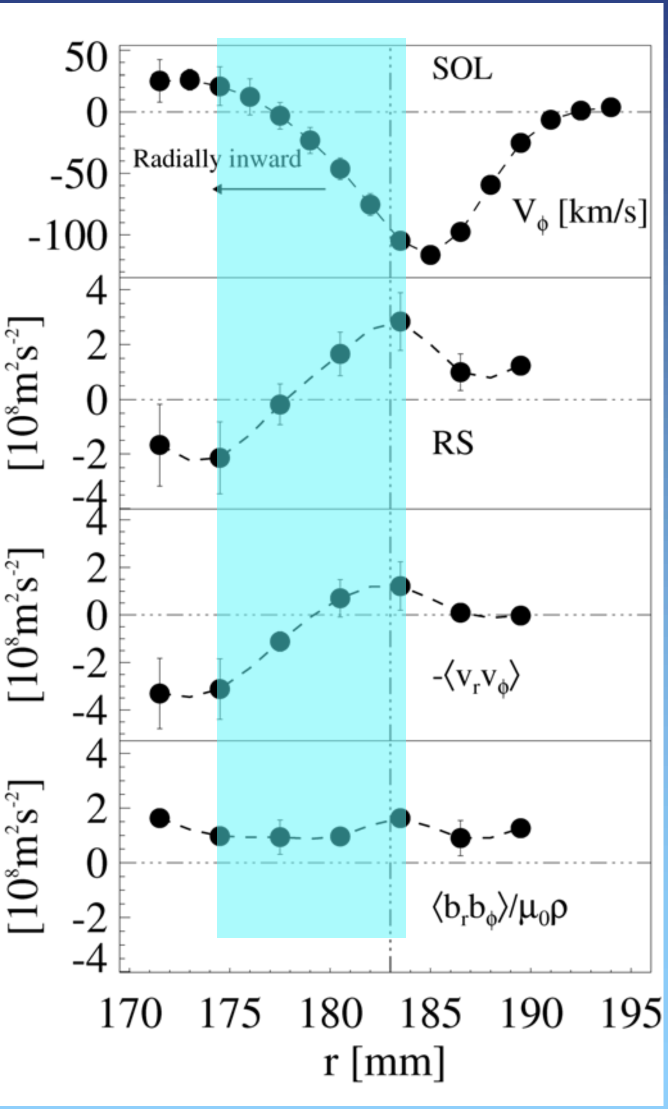

Momentum balance

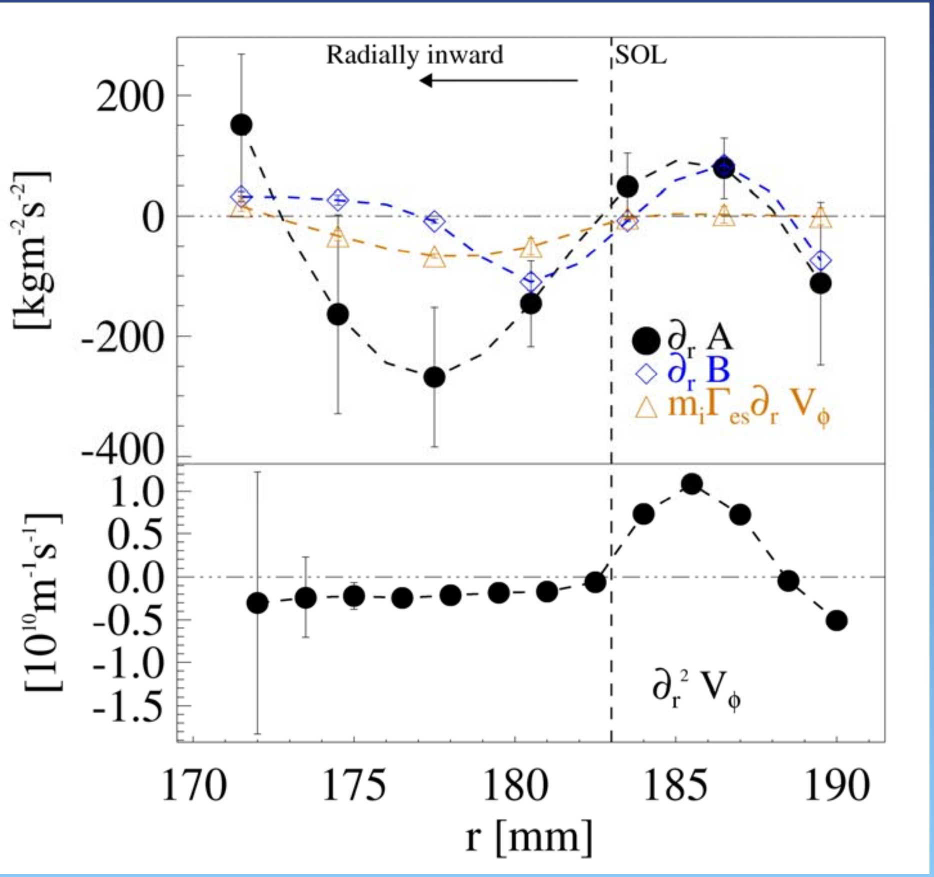

$$A = -\overline{\rho}\langle \frac{\tilde{b}_r \tilde{b}_\phi}{\overline{\rho}\mu_0} - \tilde{v}_r \tilde{v}_\phi \rangle$$

$$B = \langle \tilde{v}_r \tilde{v}_\phi \tilde{\rho} \rangle$$

$$C = m_i \Gamma_{es} \frac{\partial \overline{V}_\phi}{\partial r}$$

All terms have the same sign of velocity second derivative apart term B which acts as damping for $r \leq 178$.

Reynolds Stress (RS) is the dominant driving term inside LCFS
Electrostatic RS drives the ExB shear (as in tok and stell.)

Viscosity estimate

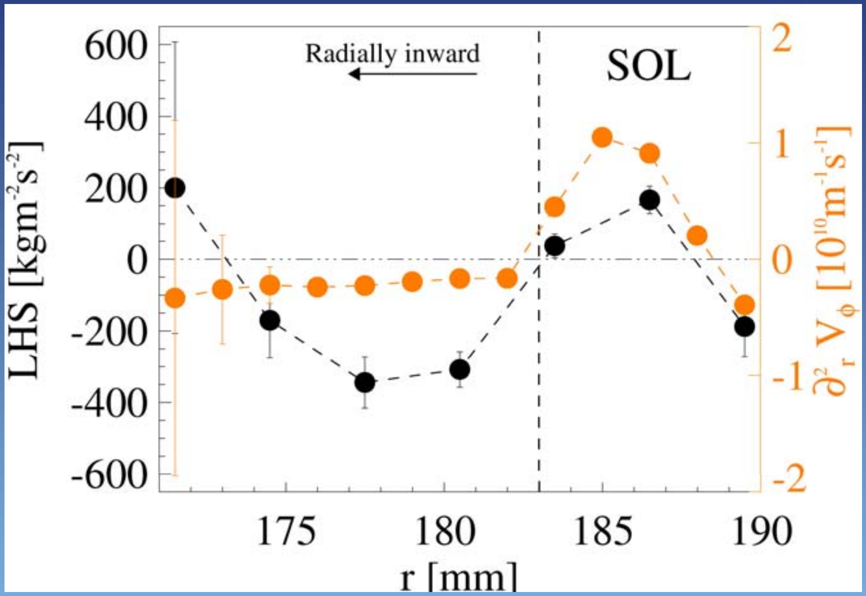

LHS and RHS of balance equation change sign in the same location across LCFS. From their ratio the perpendicular viscosity can be obtained.

$$\frac{\partial}{\partial r}\left[\underbrace{-\bar{\rho}\langle\frac{\tilde{b}_r\tilde{b}_\phi}{\bar{\rho}\mu_0}-\tilde{v}_r\tilde{v}_\phi\rangle}_{A}+\underbrace{\langle\tilde{v}_r\tilde{v}_\phi\tilde{\rho}\rangle}_{B}\right]+\underbrace{m_i\Gamma_{es}\frac{\partial\overline{V}_\phi}{\partial r}}_{C}\approx\mu\frac{\partial^2\overline{V}_\phi}{\partial r^2}$$

Experimental viscosity results much larger than classical one. Assuming **μ=ρD** the corresponding diffusivity results comparable to that caused by electrostatic turbulence.

Therefore momentum transport is anomalous and consistent with anomalous particle transport

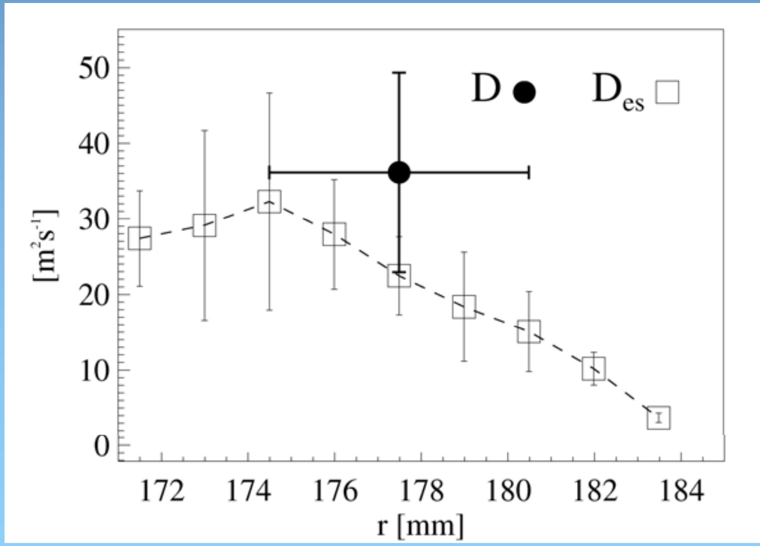

Turbulence self regulation

ExB velocity profile is the result of the balance between RS and 'anomalous' viscosity, both driven by electrostatic turbulence

The 'spontanoeus' ExB velocity shear is marginal for turbulence suppression/ mitigation

↓

A turbulence self-regulation process is in action in the edge region of RFP's

Bursts on electrostatic particle flux

Bursts are observed in primary (n,T,Φ) and derived quantities (Γ)

Γ [a.u.]

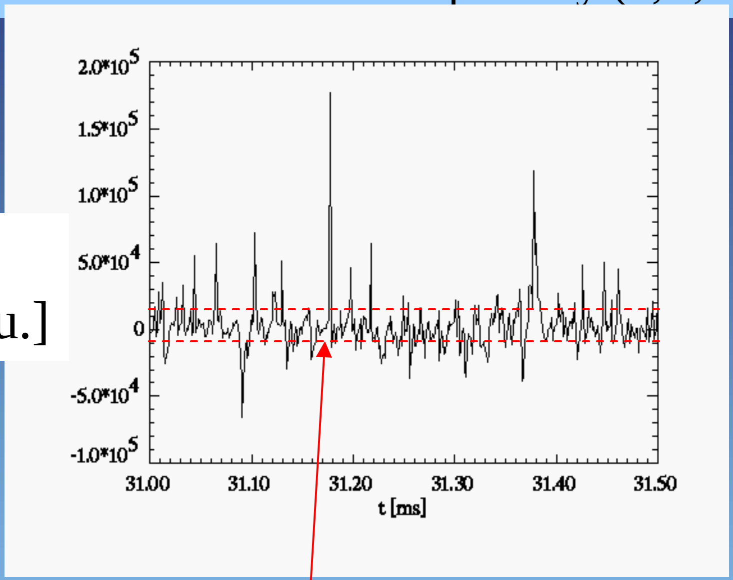

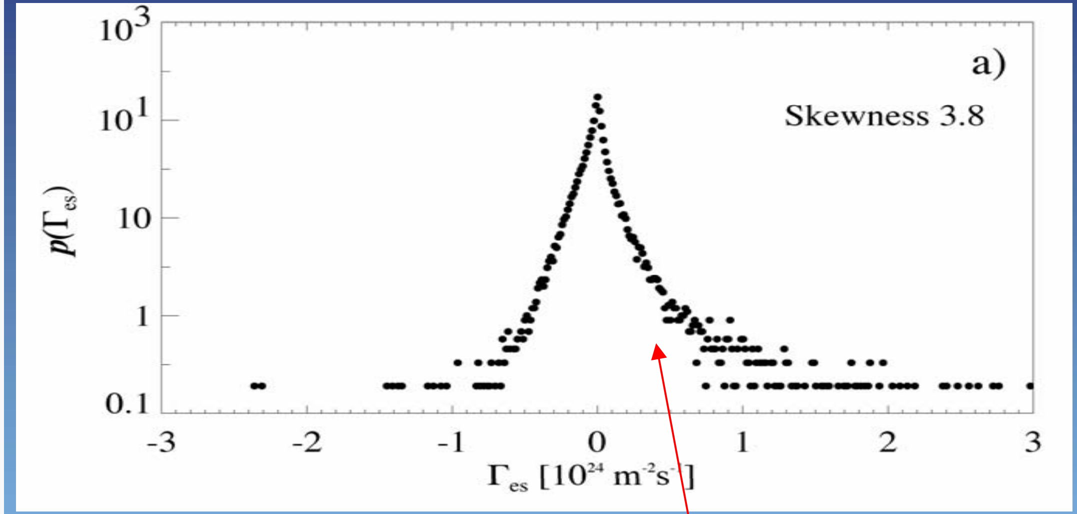

Instantaneous radial particle flux Γ_{es} (evaluated from two-point measurements) exhibits bursts and its Probability Distribution Function (PDF) is non-symmetric

Almost 50% of the particle flux is due to ‘bursts’ (as in tokamaks and stellarators)

Phys Rev Lett , 87, (2001) 045001 1-4

Statistical analysis

Wavelet analysis is applied at different time scale and a <u>Probability Distribution Function</u> of fluctuation amplitudes is calculated for each time scale τ

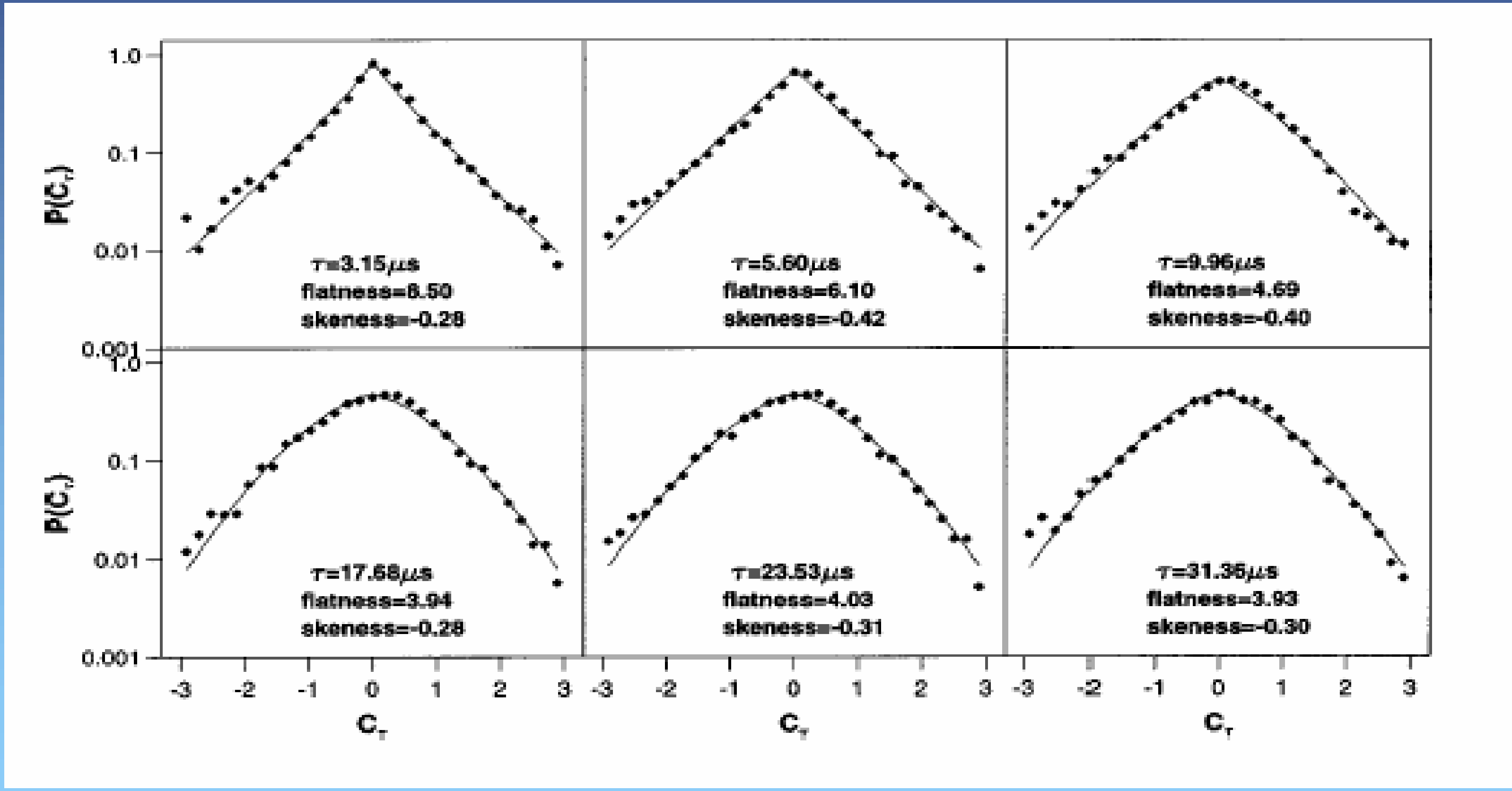

Turbulence properties: Intermittency

Wavelet analysis is applied at different time scale and a Probability Distribution Function of fluctuation amplitudes is calculated for each time scale τ

Floating potential data on RFX

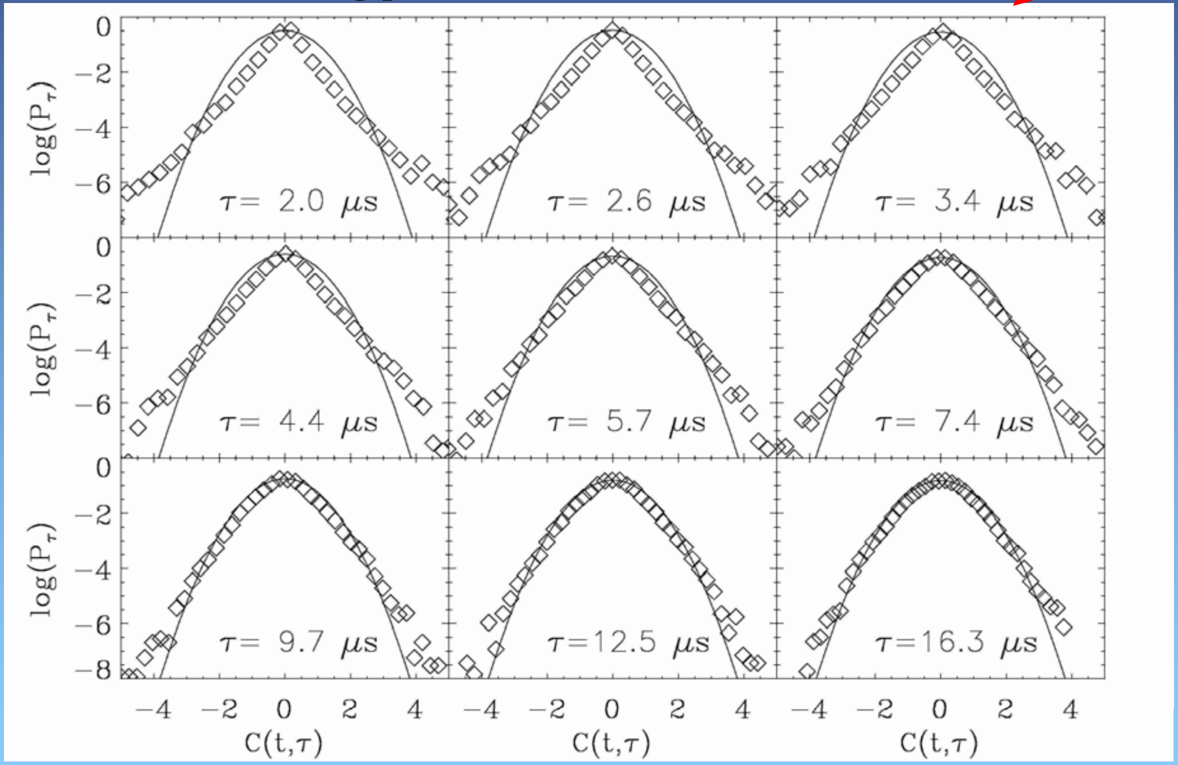

Electrostatic turbulence in RFX and T2R exhibits non-gaussian tails at short time scales in primary and derived quantities

- In turbulent fluids intermittency manifests itself as a departure from self-similarity in the Probability Distribution Function (PDF) and power law in PDF momentum

U. Frisch, *Turbulence: The legacy of A. N. Kolmogorov*, Cambridge University Press, Cambridge 1995

Phys.Plasmas 7, 445 (2000)

Bursts belong to the non-gaussian tail of the PDF and (in RFP) have intermittent character

Intermittency in magnetic turbulence and particle flux

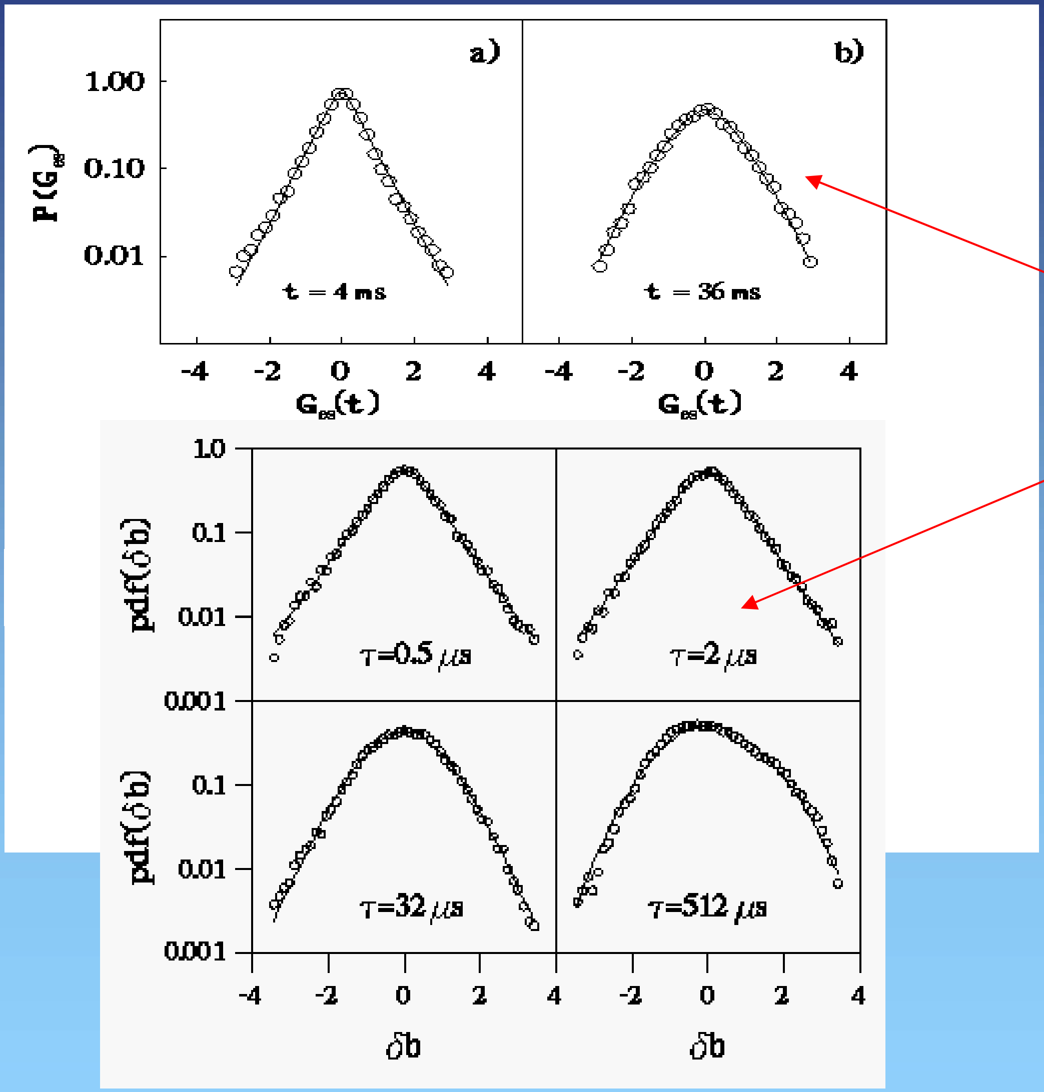

Intermittency has been found in:

particle flux

and

magnetic turbulence.

Phys.Rev E 62, R49 (2000)

Intermittent event features

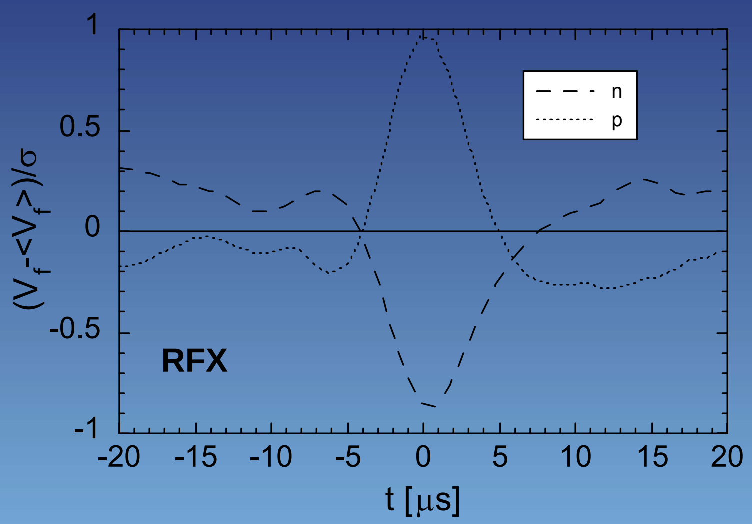

Bursts (negative and positive) in raw signals of V_f have been sorted out from background turbulence and analysed by conditional average .

The (normalized) average time structure for minima or maxima has been obtained.

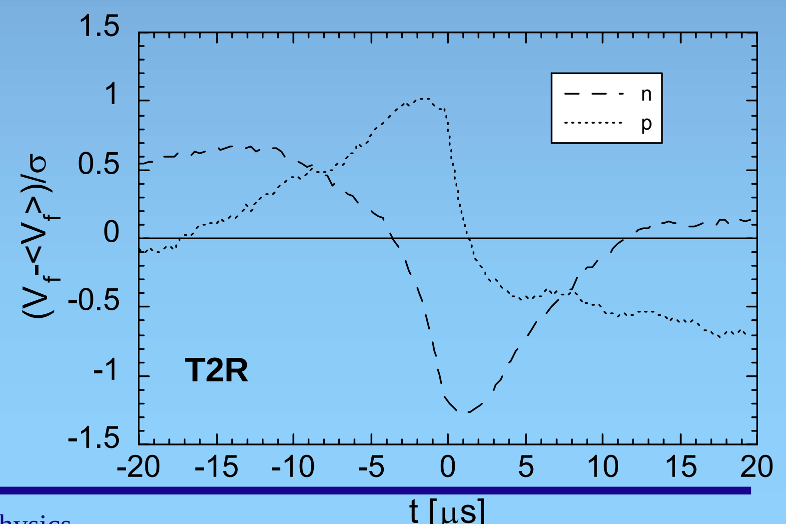

2D reconstruction

By radial array of probes, the V_f (r,t) structure associated to local minima and maxima has been reconstructed

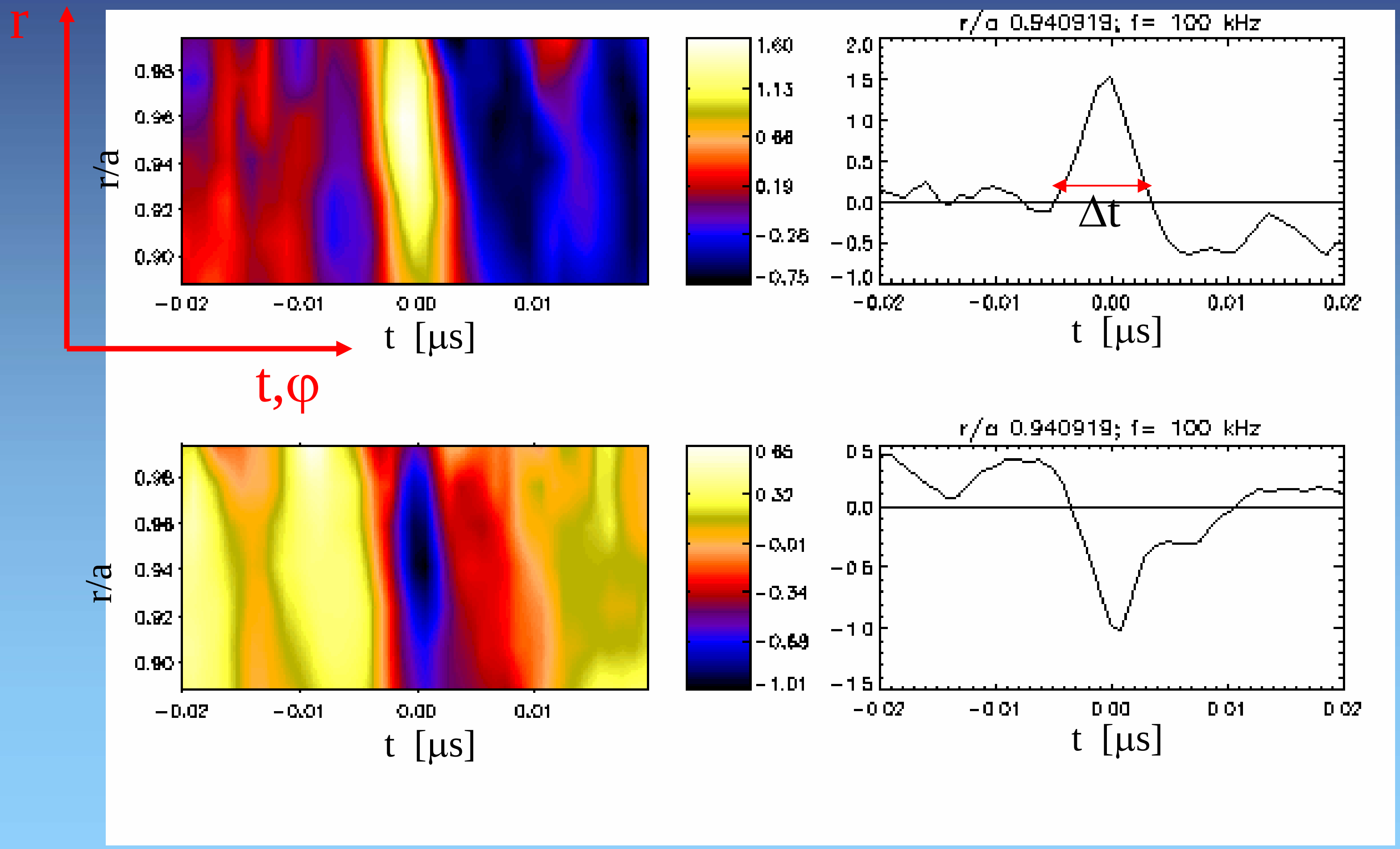

Intermittent events and structures

Structures associated to intermittent events have been reconstructed by using radial arrays of probes (*rake)* and Taylor's hypothesis (frozen turbulence)

RFX

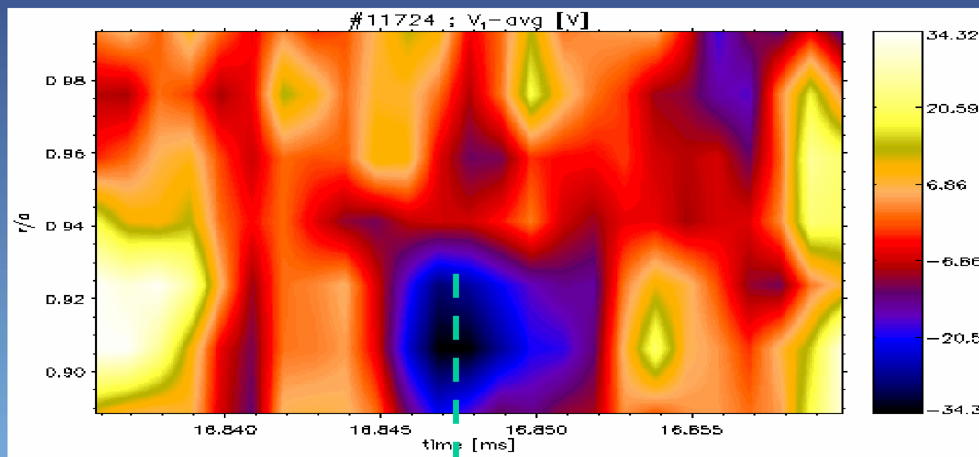

from plasma potential time behaviour...

…through ExB mean velocity ...

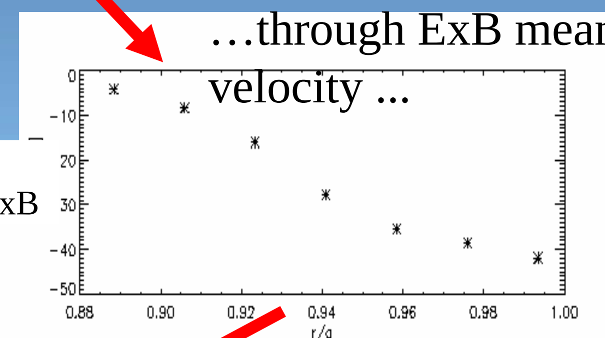

intermittent event

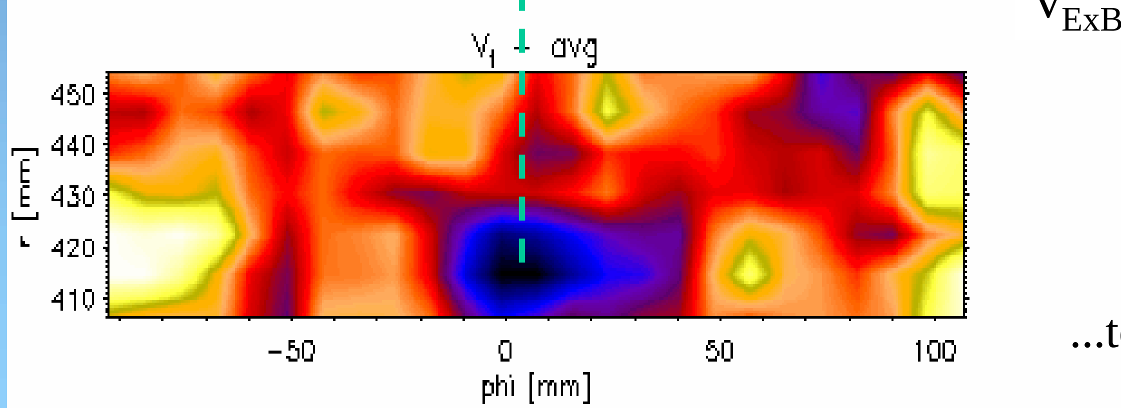

...to potential spatial structure...

Intermittent events and structures

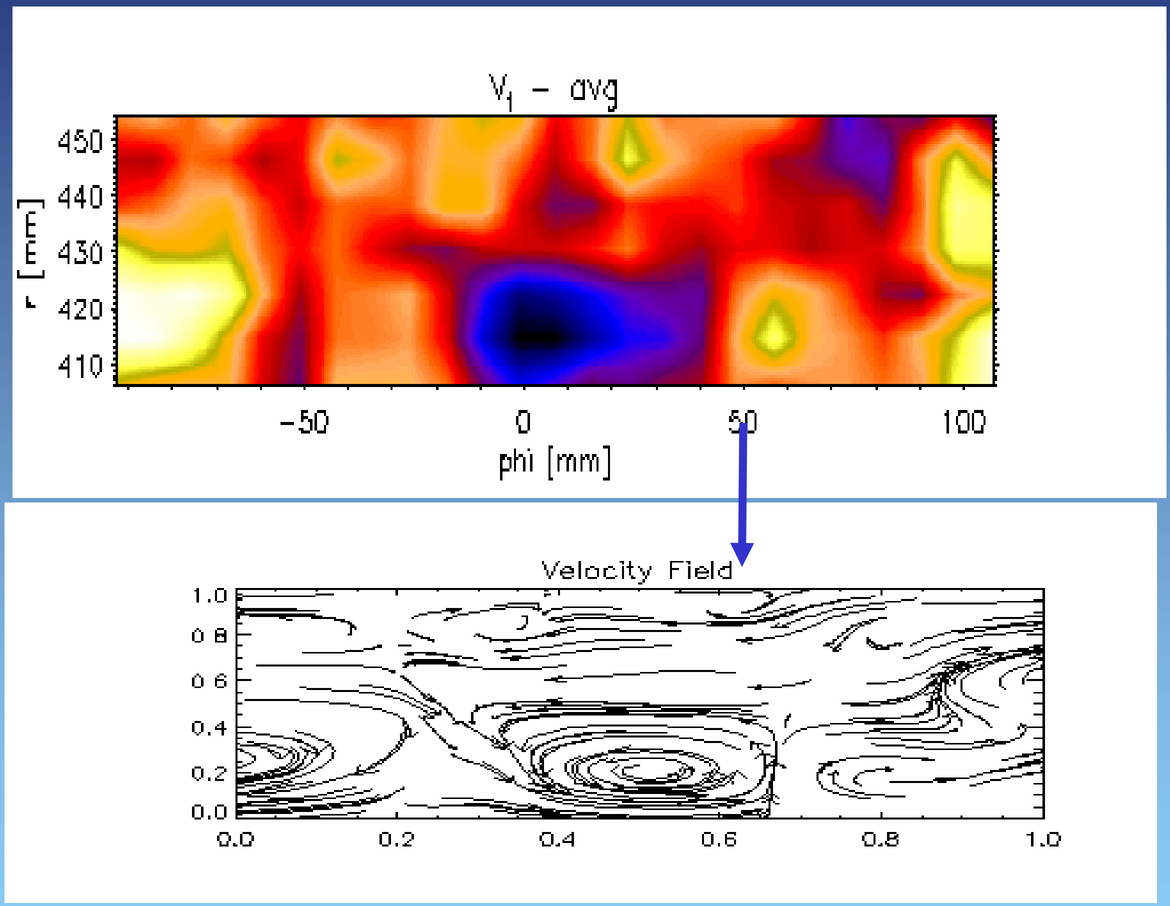

...to electric field spatial structure...

...to ExB velocity pattern...

Structures look like vortices propagating with toroidal velocity v_{ExB}~10 km/s (in RFX) and with toroidal extension $\Delta t \cdot v_{ExB}$~10 cm and radial extension~3cm

Bursts and vortices

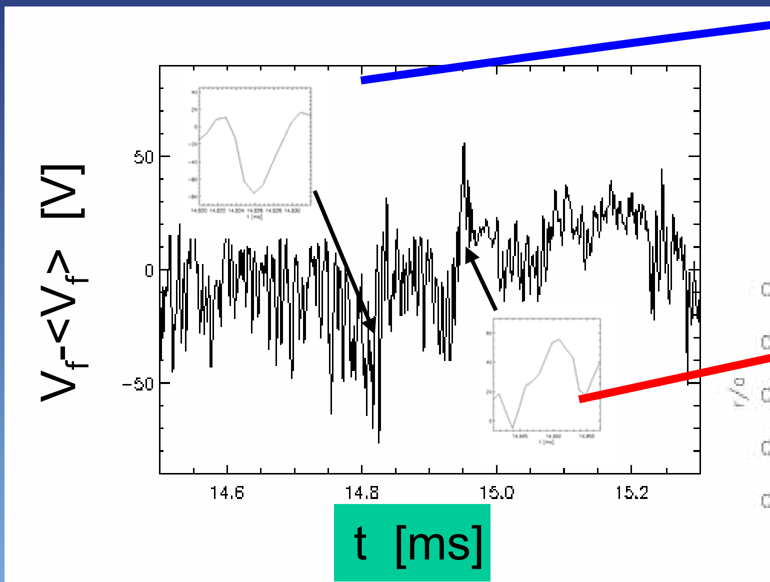

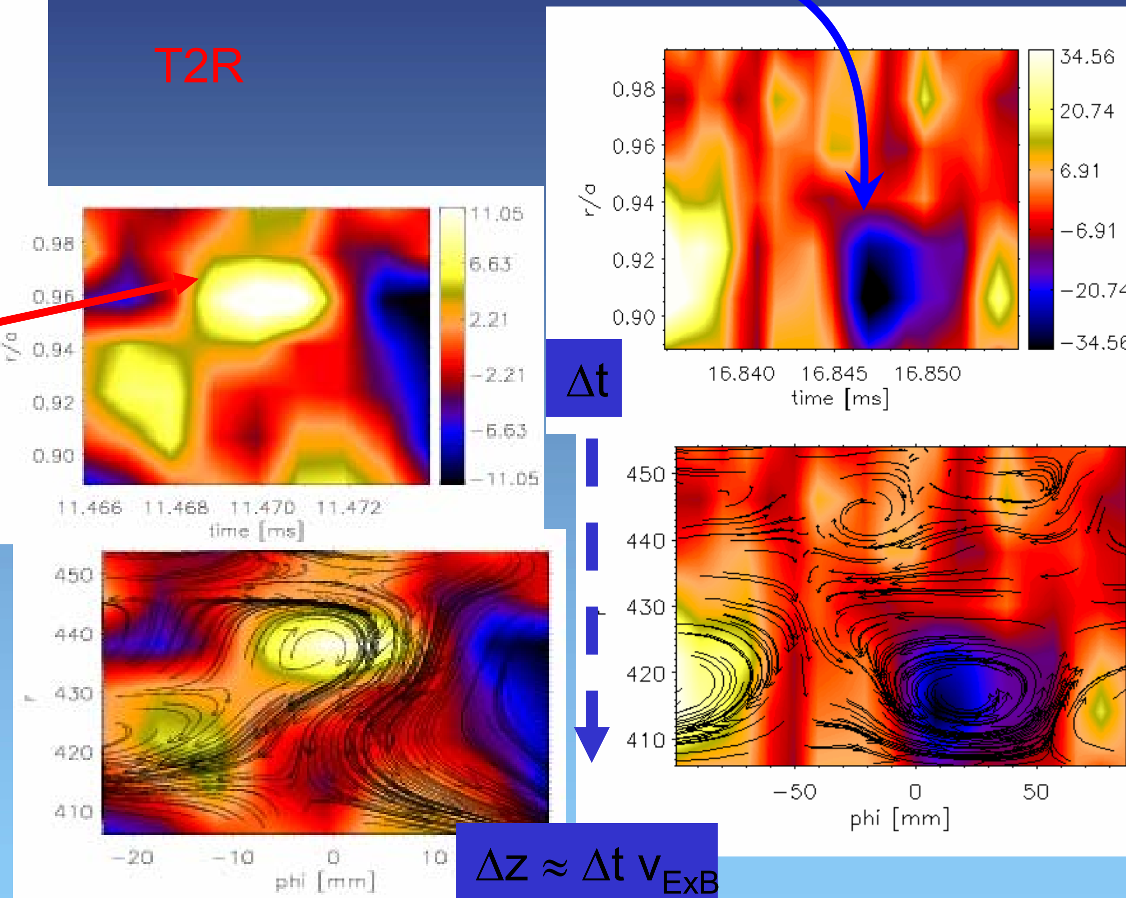

Bursts in V_f correspond to vortices with opposite vorticity

Numerical simulation

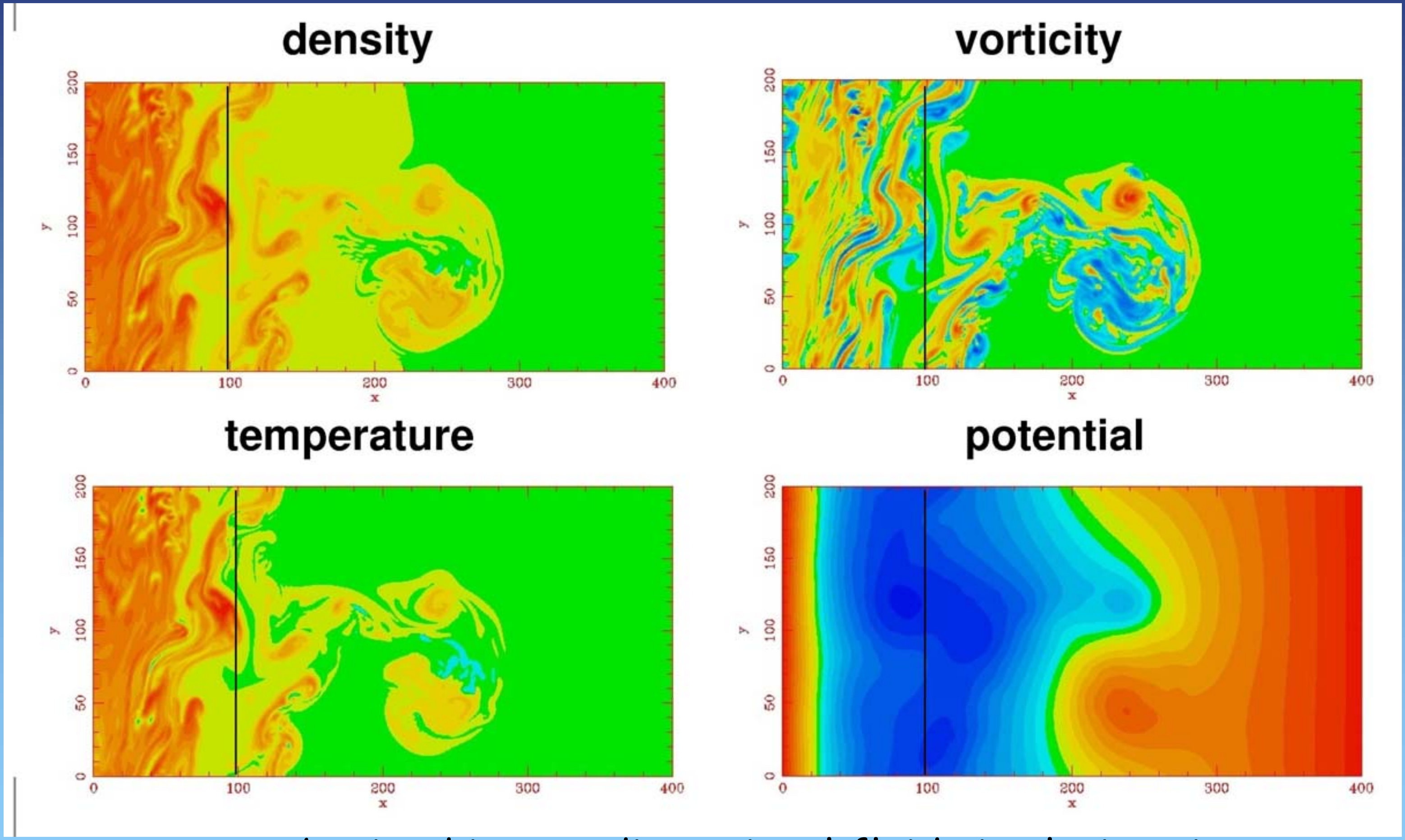

Similar structures obtained in two-dimensional fluid simulations in scrape-off layer of magnetized plasmas.(O. E. Garcia,V. Naulin, A. H. Nielsen, and J. Juul Rasmussen PRL 92(2004), 165003-1)

Numerical simulation

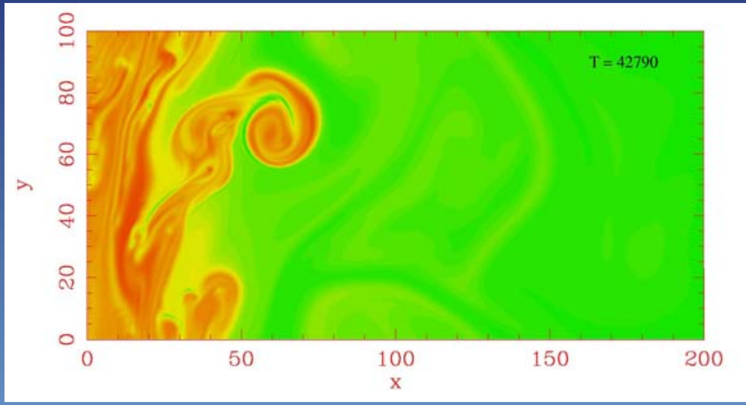

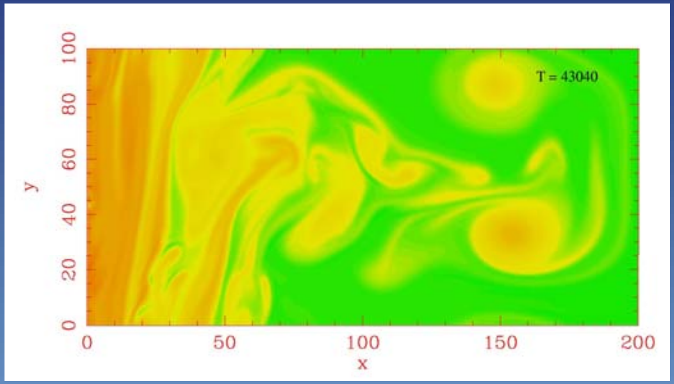

…example of blob propagation

Simulations also predict the same statistical properties (bursts, non symmetric PDF,…)

Dipolar vortices

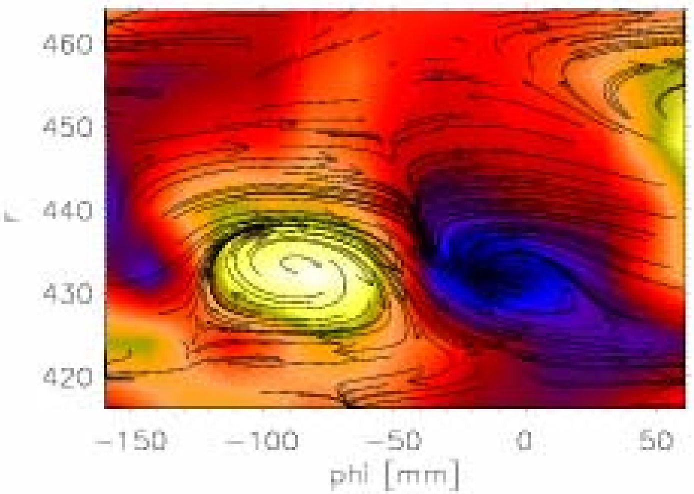

Reconstruction of a structure observed in a low shear region (RFX)

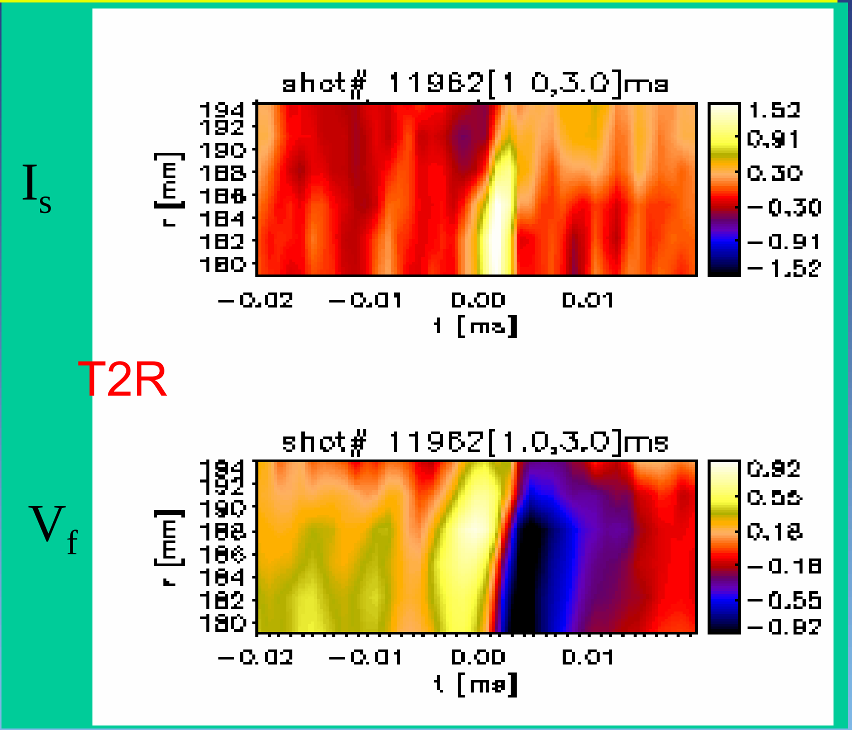

Estimate of dipolar/monopolar vortices population:

<u>Hypothesis</u>:
positive and negative structures combine to maximize the dipolar vortices population

$$N_{mono} = |N_p - N_n|$$ **monopolar** structures

$$N_{dip} = (N_p + N_n - N_{mono})/2$$ **dipolar** structures

Vortices population and ExB shear

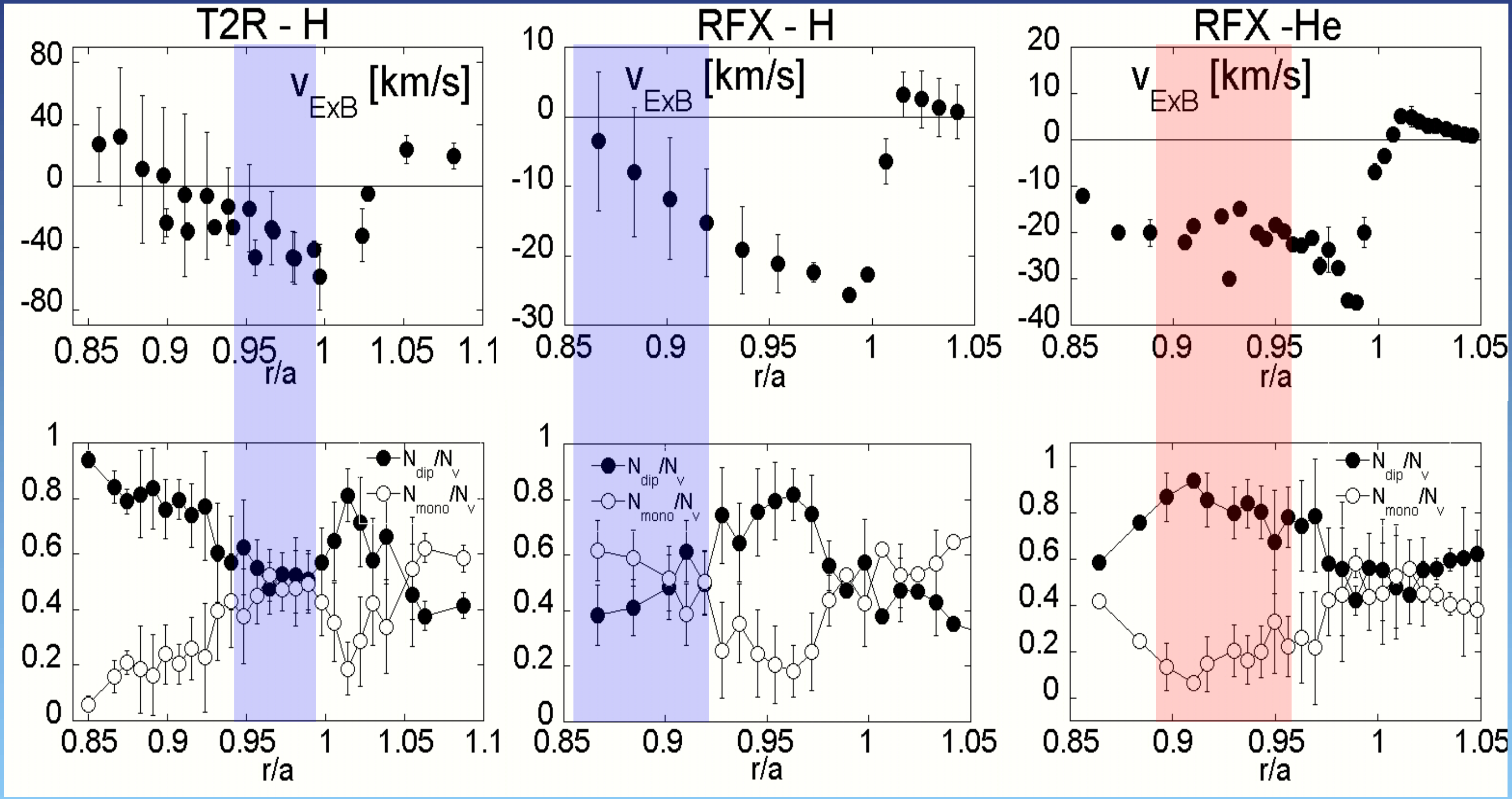

Dipolar vortices constitute the **larger** population where the v_{ExB} shear is lower and tend to **decrease** in higher shear regions

Vortices and transport

Horton-Ichikawa's model

$$D = D_v + D_{background}$$

$$D_{background} = D_{Bohm} = \frac{1}{16}\frac{T}{B}$$

$$D_v = r_0 v_d f_v^{\,2}$$

r_0 vortex radius
v_d vortex velocity
f_v packing fraction

A contribute to anomalous diffusion is due to vortex interactions through:

•displacement of structures

•rearrangement of vorticity patterns lead to faster spreading and escape of advected particles

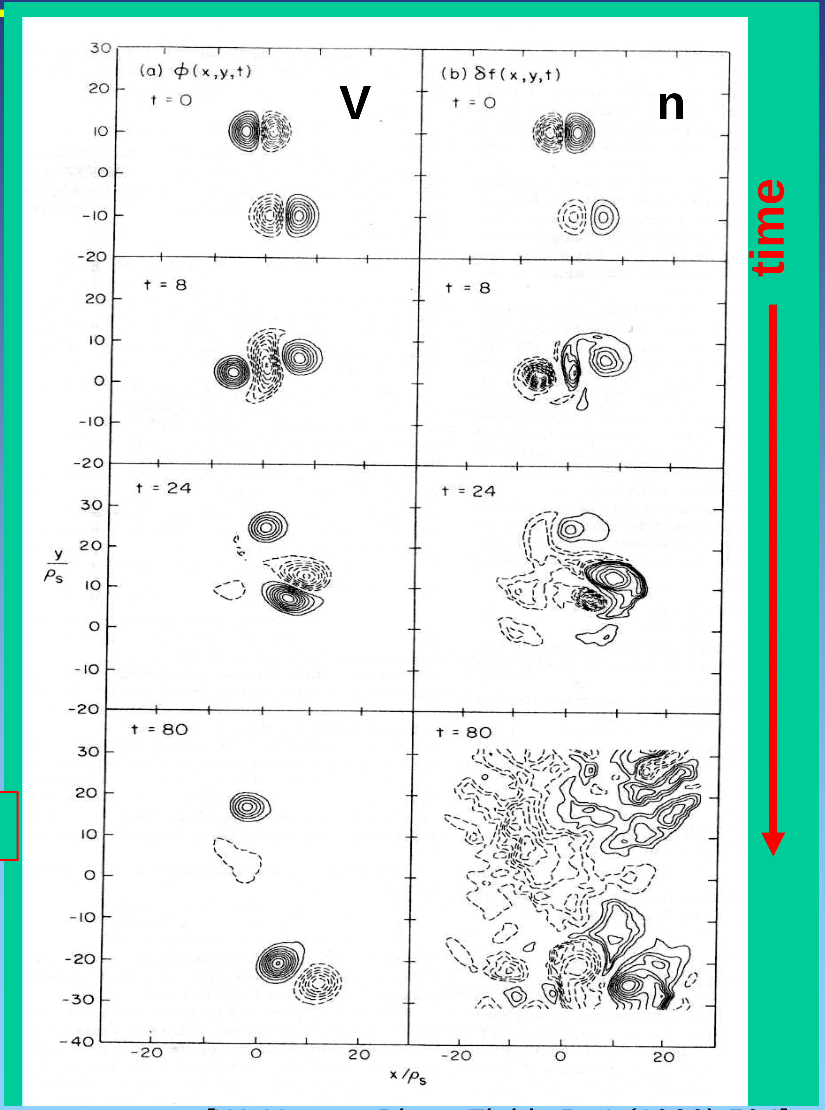

[W. Horton, Phys. Fluids B, 1 (1989) 524]

Estimate of the packing fraction

$$f_v(r,\tau) = \frac{N_v(r,\tau)S_v(r,\tau)}{S_T(r)} \cong \frac{N_v(r,\tau)\Delta r \Delta z}{2\pi(R+r)\Delta r}$$

$$f_v(r) = f_d(r) + f_m(r)$$

Coherent structures occupies 20-30% of the space in the edge region

$$D = D_v + (1 - f_v)\ D_{Bohm}$$

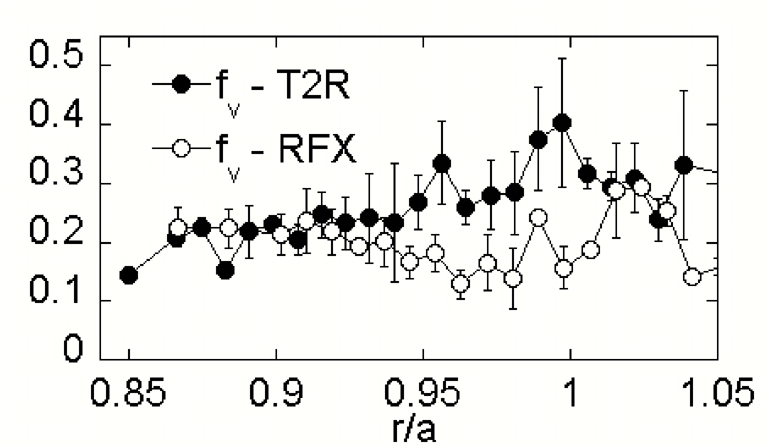

Experimental estimate of D_v

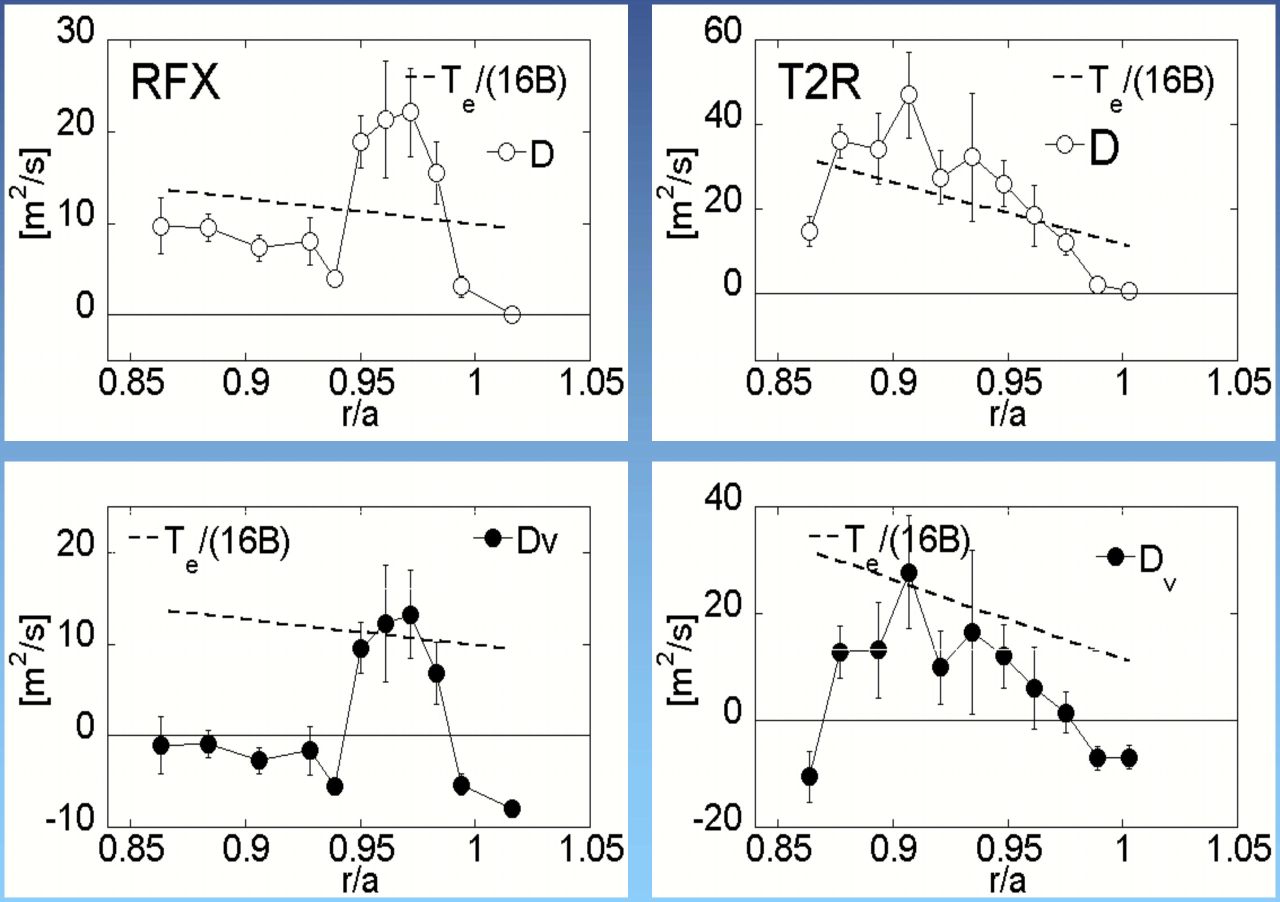

In the outer region of RFX and T2R:

$$D = -\Gamma_{es} / \nabla n \geq D_{Bohm}$$

D_v accounts for up to 50% of the experimental total diffusivity D

Vortices and diffusivity

$$D_v = r_0 v_d \left(\alpha \; f_d^{\,2} + \beta \; f_d f_m + \gamma \; f_m^{\,2}\right)$$

Generalization of Horton's formula

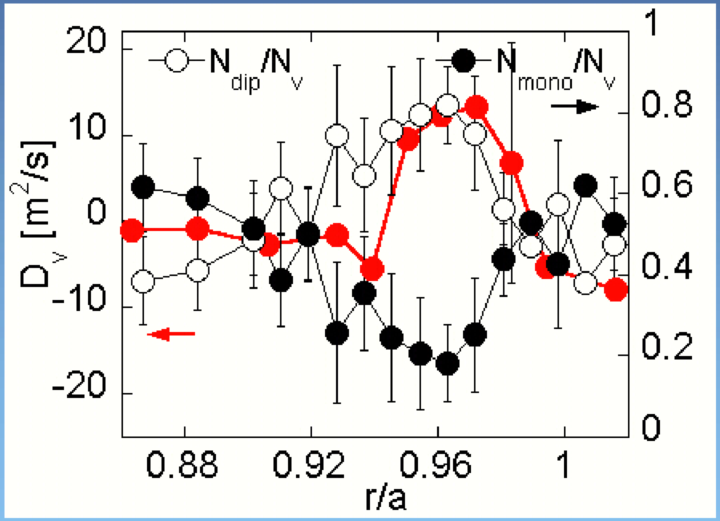

The polynomial can be simplified as :

$$D_v \approx \alpha r_0 v_d \left(f_d - 2 f_m\right)^2$$

In RFX and T2R, D_v minimum where $f_d \approx 2f_m$ i.e. were the two populations are equal

NB. Analogous to Horton's formula for f_m=0 and $\alpha \approx 1$

$$D_v = r_0 v_d \, f_v^{\,2}$$

Comparison with experimental results

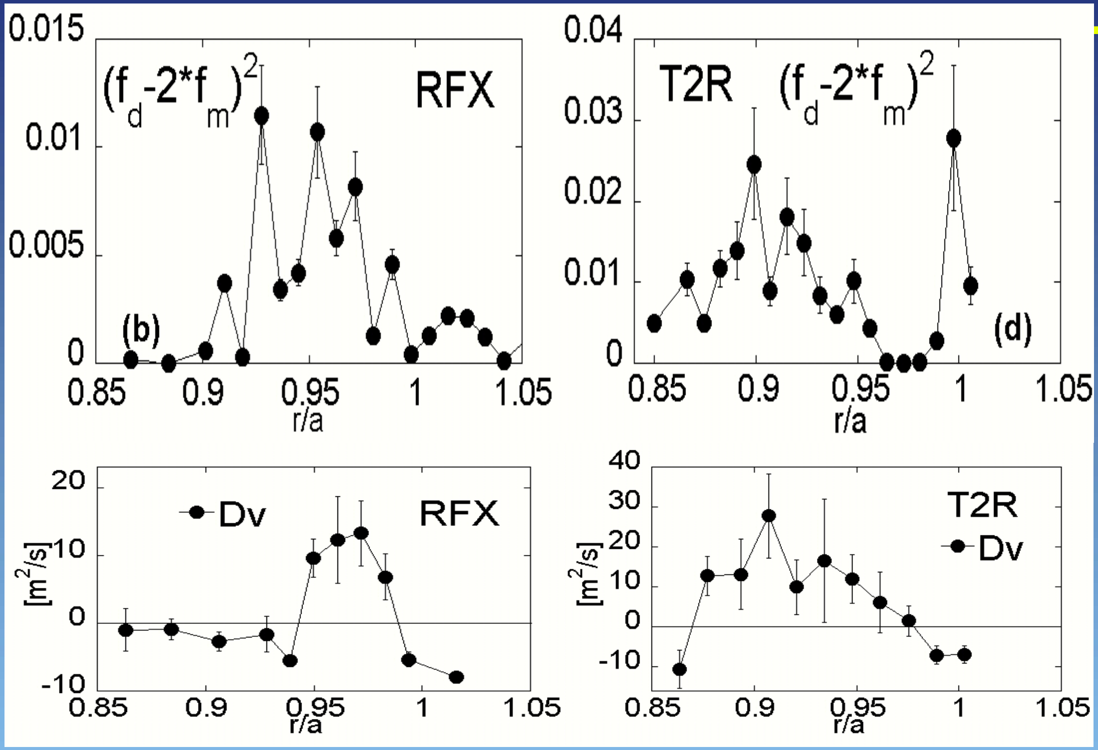

In both experiments the term $(f_d - 2f_m)^2$ tracks fairly well the spatial behavior of D_v

$$D_v \approx r_0 v_d \left(f_d - 2 f_m \right)^2$$

Estimate of v_d where D_v is at maximum:

$$v_d \approx \frac{r_0 \left(f_d - 2 f_m \right)^2}{D_v}$$

$$r_0 \approx \sqrt{\Delta r \, \Delta z} \big/ 2$$

$v_d \approx 20 – 30$ km/s

Consistent with v_{ExB} drift velocity

To be published in Phys. Rev. Lett.

Coherent structures and transport

50% of particle transport is due to interaction of vortex-like structures travelling with a velocity close to ExB drift velocity and occupying 20% of the space in the edge region

Intermittency & Magnetic Relaxation

By an iterative procedure called Local Intermittency Measurement*, fluctuations are wavelet decomposed and for each time scale τ an amplitude threshold is identified to sort out the *intermittent events* from the Gaussian background

**M.Onorato et al., Phys.Rev E 61, 1447 (2000),*

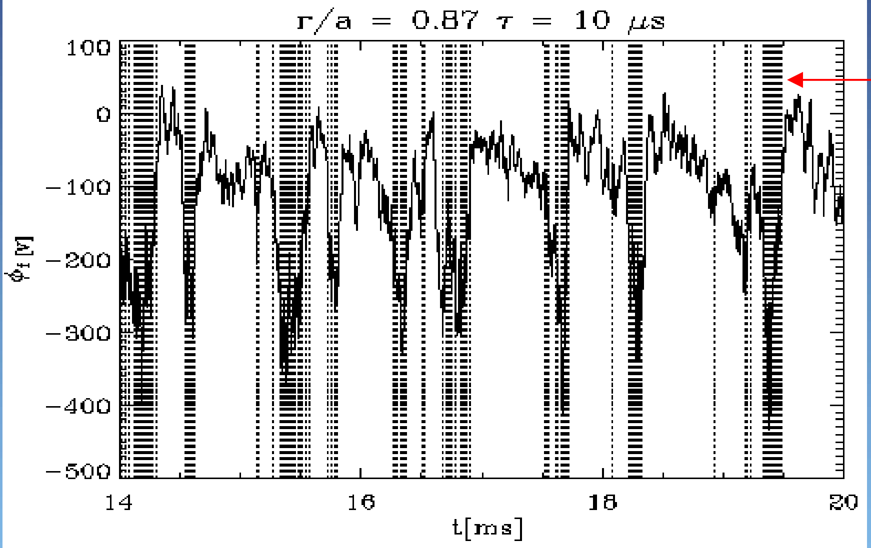

RFX

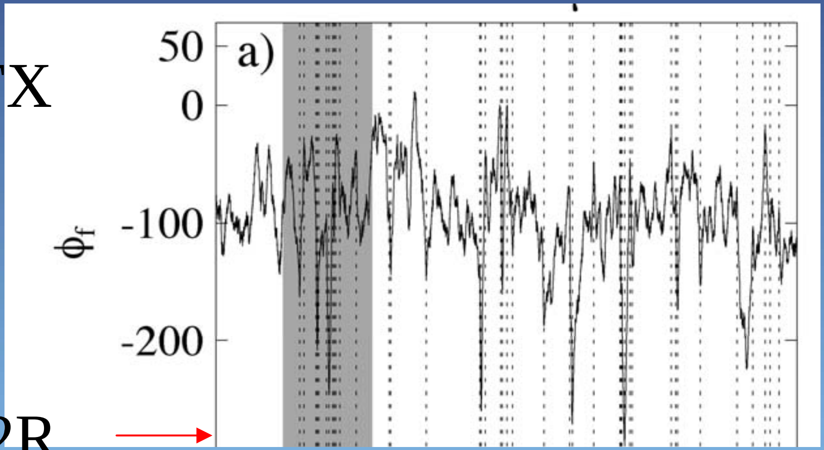

T2R

In RFX and T2R intermittent events tend to cluster at the occurrence of *minima* in the mean plasma potential.
As these *minima* are correlated with cyclic magnetic relaxation, a non-linear coupling between core MHD modes and edge electrostatic turbulence is proved.

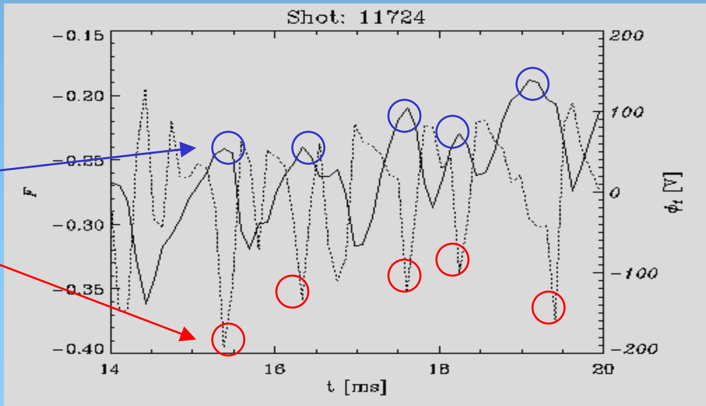

Europhys. Lett. 54 (2001)51
PPCF 44 (2002) 2513

Turbulence control: techniques

Turbulent transport reduction by modification of the ExB flow shear has been achieved:

in RFX by Edge biasing

In T2R by Pulsed Poloidal Current Drive (PPCD)

Turbulence control:edge biasing

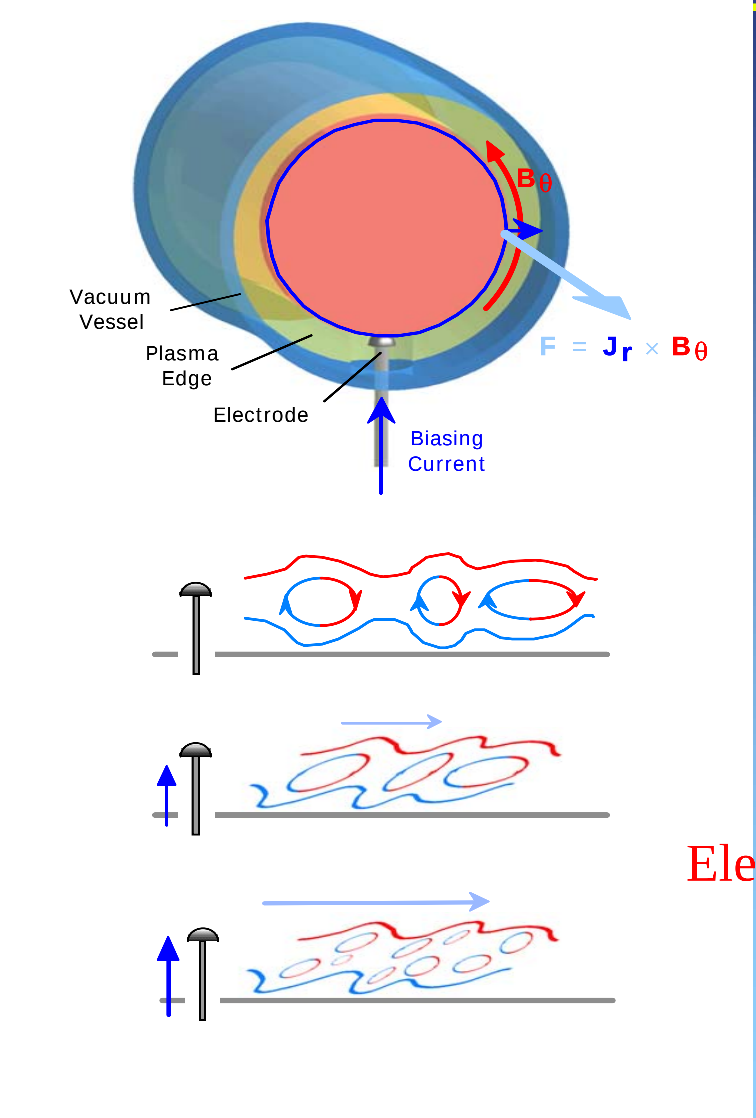

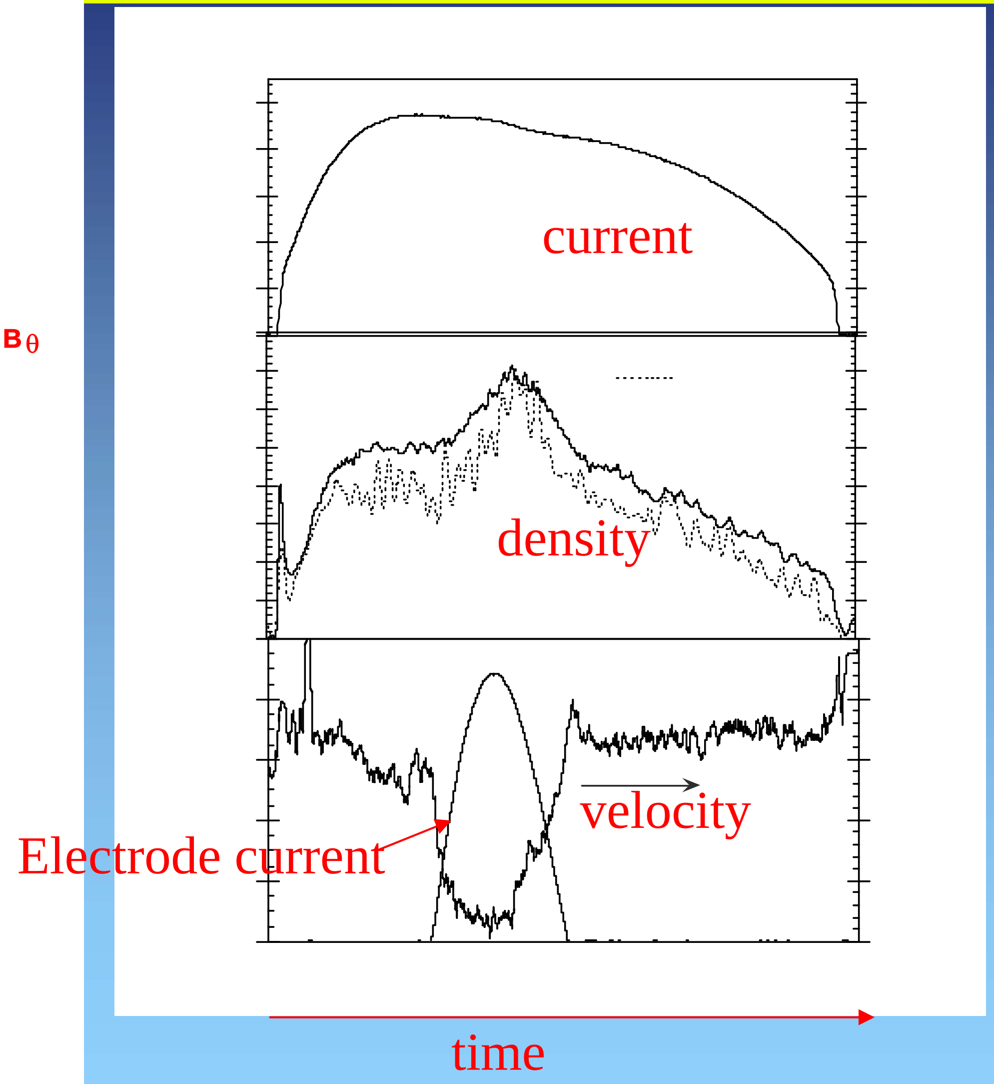

Turbulence control:edge biasing

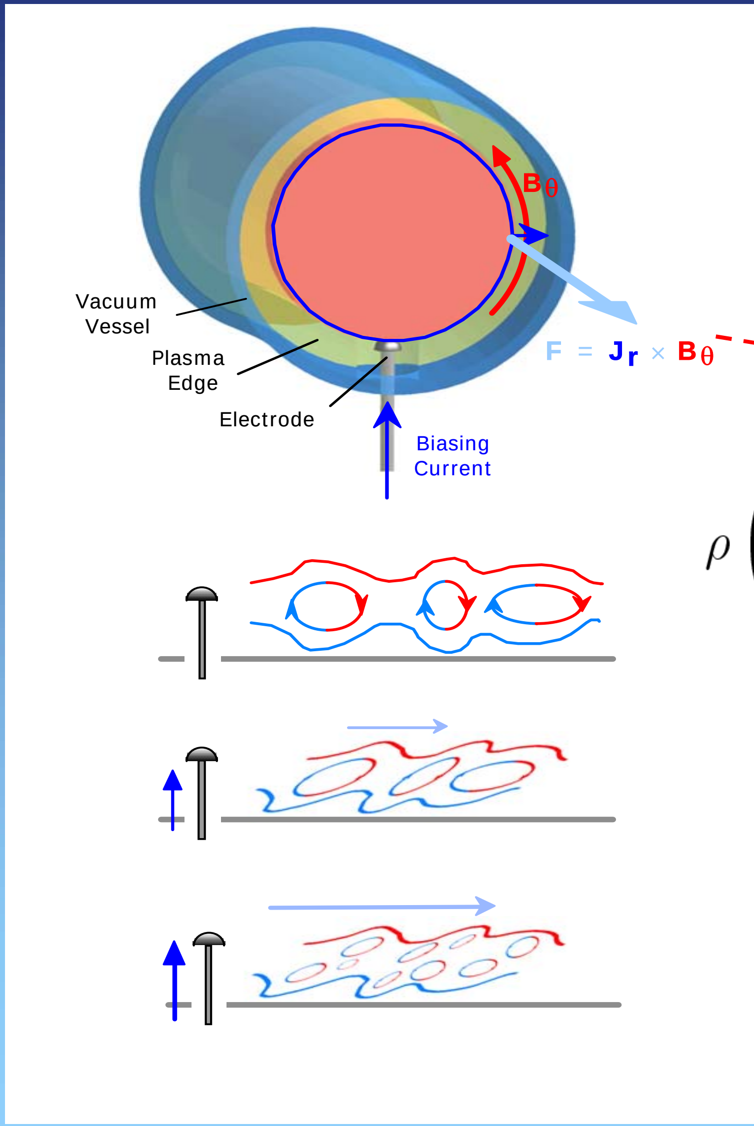

$$\rho\left(\frac{\partial}{\partial t} + \mathbf{V}\cdot\nabla\right)\mathbf{V} = -\nabla\mathbf{P} + \mu\nabla^2\mathbf{V} + \mathbf{J}\times\mathbf{B}$$

Momentum equation

V Antoni, et al. Plasma Phys. Control. Fusion **42** (2000) 83–90

Turbulence control:edge biasing

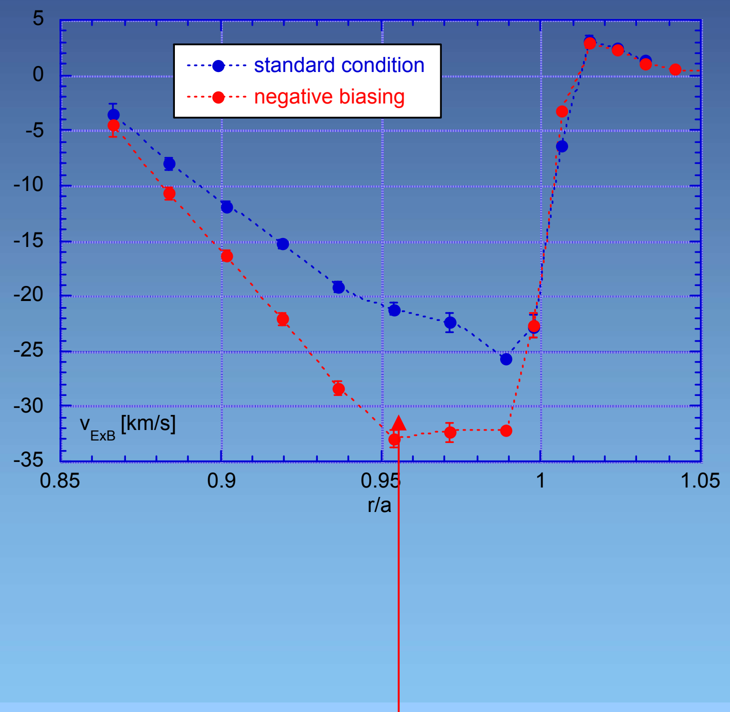

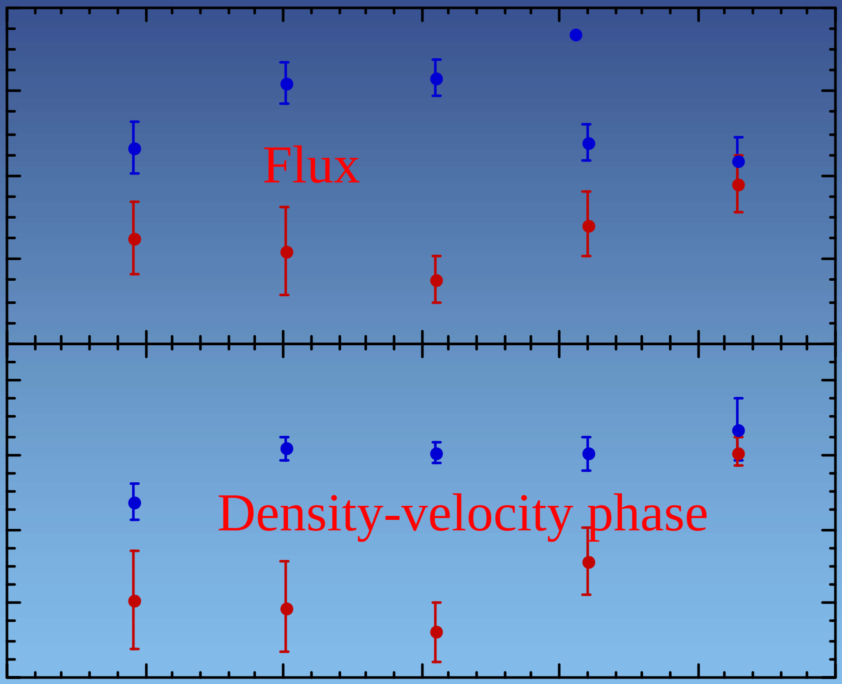

Increasing the ExB velocity shear the particle flux (and D) decreases and the reduction is mainly due to a modification of density and velocity fluctuation cross-phase, as observed in other experiments and predicted by theory in some case (P.W. Terry, et al ,Phys Rev Lett , **87**,(2001) 185001-1)

Plasma Phys. Control. Fusion 42 (2000) 83–90

Turbulence control:edge biasing

the particle flux decreases…

…mainly by phase shift and decorrelation…

…not by turbulence suppression

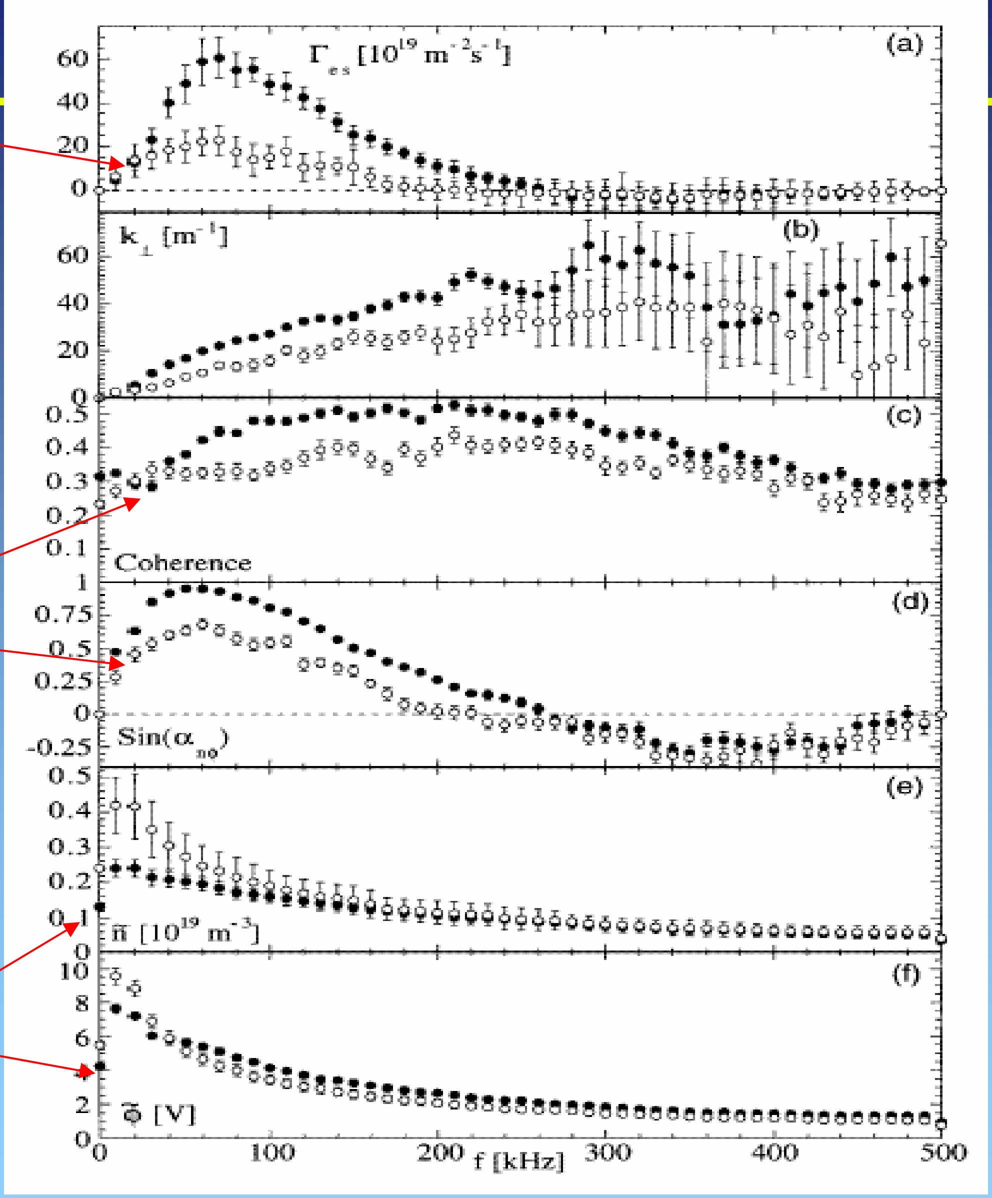

Turbulence control: pulsed poloidal current drive

In T2R a transient poloidal electric field can be applied by a fast change of the toroidal field. This technique is called Pulsed Poloidal Current Drive (PPCD)

A steep (10-fold) increase of the toroidal ExB flow shear is observed

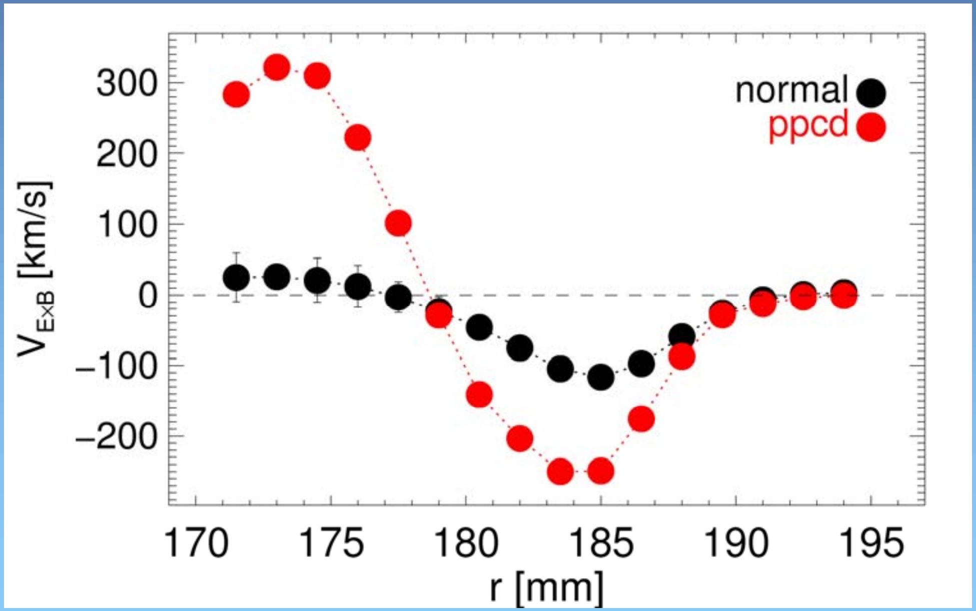

Turbulence control: pulsed poloidal current drive

A reduction of the burst intensity is observed → reduction of structure's vorticity

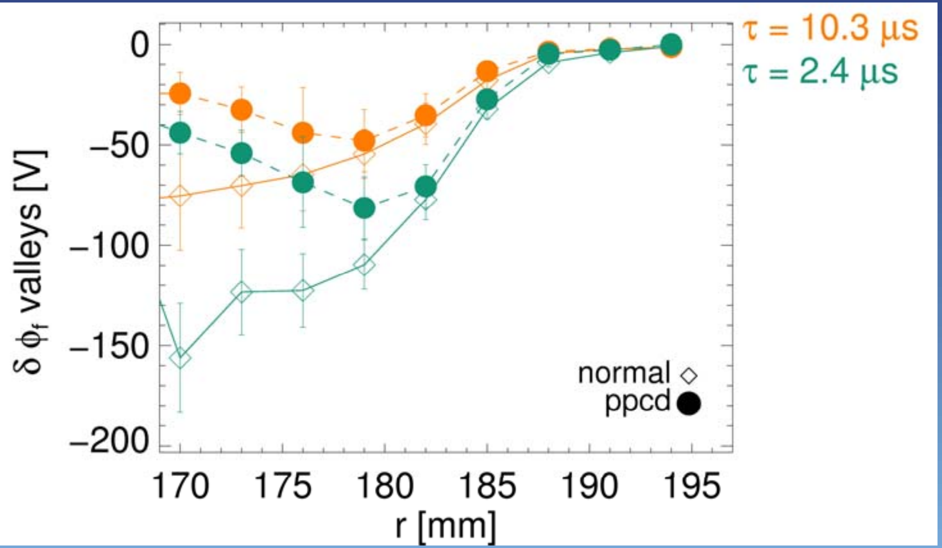

No clear evidence of reduction in number in the region where the shear increases

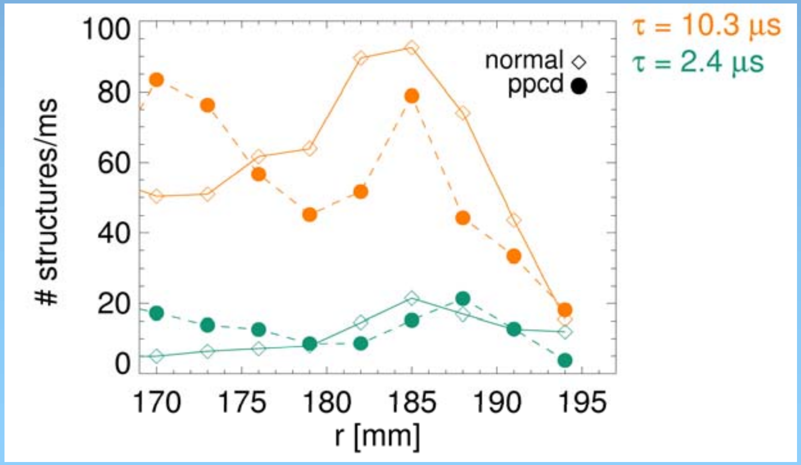

Work in progress

Scientific program for MHD control in RFX

RFX plasma experiments will restart by the end of 2004.

The scientific programme aims at enhancing plasma confinement and among
the main topics is the MHD control.

New tools will be available for:

-Driven rotation of MHD modes;

-Controlled formation of Quasi-Single Helicity states by driving helical fields atthe plasma boundary;

-Feedback stabilization of Resistive Wall Modes;

- Simultaneous control of equilibrium, helical fields and rotating m=0 perturbations.

Tools for MHD control

New tools to allow a direct magnetic interaction with the m=1 and m=0 modes :
- Replacement of the thick shell with a much thinner one (τ <50ms);
- Installation of a new system of 192 (4x48) saddle coils, individually fed by fast amplifiers (switching frequency 10 kHz);
- Improvement of the toroidal field power supply;
- Improvement of magnetic measurements (192 B_r, 192 B_ϕ,B_Θ.

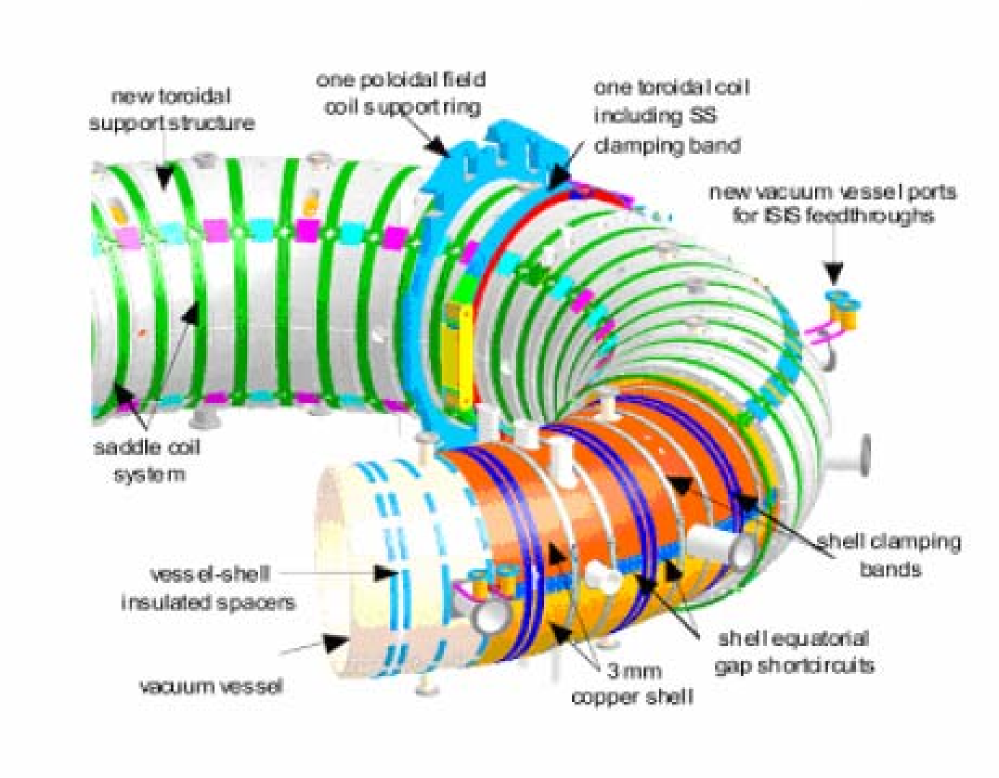

Conclusions

A turbulence self-regulation process is in action in the edge region of RFP's.
The highly sheared ExB flow at the edge comes from a balance between Reynolds stress and anomalous viscosity, both mainly driven by electrostatic turbulence

Coherent structures emerge from the turbulent background. They diffuse and interact in a highly sheared flow velocity region and as a result they contribute to 50% of the particle transport.

Turbulence control experiments show that externally induced high flow shear can reduce the transport due to background and structures.

As RFP edge physics shows several analogies with other configurations, investigation of magnetic and electrostatic turbulence in this configuration can contribute to general advance of fusion research.
Studies on MHD control will be relevant also for Tokamaks operating under advanced confinement scenarios.

Aknowledgments

This work has been made possible thanks to the work and contributions of several colleagues of RFX and EXTRAP-T2R teams and in particular:
R. Cavazzana, S. Cappello, E. Martines, G. Regnoli(a), G. Serianni, E. Spada, M. Spolaore, N. Vianello, J. Drake (b), H. Bergsåker(b), M. Cecconello (b)

Consorzio RFX, Associazione Euratom_ENEA sulla Fusione, Italy
(a) ENEA,Frascati, Italy
(b)*Alfvèn Laboratory, Royal Institut of Technology, Association EURATOM/NFR, Stockholm, Sweden*

Special thanks to V. Naulin and J. Juul Rasmussen for material on numerical simulations
Association EURATOM-Risø National Laboratory, Denmark